

latheo, a *Drosophila* Gene Involved in Learning, Regulates Functional Synaptic Plasticity

Jeffrey Rohrbough,* Shirly Pinto,^{†‡}
Robert M. Mihalek,^{†§} Tim Tully,^{†§}
and Kendal Broadie*^{||}

*Department of Biology
University of Utah

Salt Lake City, Utah 84112

[†]Center for Learning and Memory
Cold Spring Harbor Laboratory
Cold Spring Harbor, New York 11724

[‡]Neuroscience Graduate Program
Joan and Sanford I. Weill Graduate School
of Medical Sciences

Cornell University
New York, New York 10021

[§]Department of Biology
Brandeis University
Waltham, Massachusetts 02254

Summary

Mutations in the *latheo* (*lat*) gene disrupt associative learning in *Drosophila*, but a role for LAT in regulating neuronal function has not been demonstrated. Here, we report that LAT plays a central role in regulating Ca²⁺- and activity-dependent synaptic plasticity. Immunological localization of the LAT protein indicates it is present at synaptic connections of the larval neuromuscular junction (NMJ) and is enriched in presynaptic boutons. Basal synaptic transmission amplitude at the *lat* mutant NMJ is elevated 3- to 4-fold, and Ca²⁺ dependence of transmission is significantly reduced. Multiple forms of synaptic facilitation and posttetanic potentiation (PTP) are strongly depressed or absent at the mutant synapse. Our results suggest that LAT is a novel presynaptic protein with a role in the Ca²⁺-dependent synaptic modulation mechanisms necessary for behavioral plasticity.

Introduction

Cellular forms of synaptic plasticity are highly conserved at synapses in different systems and are believed to underlie distinct aspects of learning and memory in the brain (Kandel and Schwartz, 1982; Hawkins et al., 1993; Nguyen et al., 1994; Goda, 1995a, 1995b; Bailey et al., 1996; Yin and Tully, 1996). The fruit fly *Drosophila* is particularly amenable to genetic and behavioral analysis of learning as well as to physiological investigation of synaptic function. These attributes make *Drosophila* an excellent system for identifying genes involved in discrete steps of learning-to-memory processes and assaying the synaptic consequences of mutations in these

genes (Tully et al., 1994; DeZazzo and Tully, 1995; Davis, 1996; Goodwin et al., 1997; Tully, 1997; Dubnau and Tully, 1998). In particular, the *Drosophila* neuromuscular junction (NMJ) has been useful for revealing morphological and functional synaptic plasticity defects associated with known learning and memory mutants (Zhong and Wu, 1991; Delgado et al., 1992; Zhong et al., 1992; Wang et al., 1994; Davis et al., 1996; Broadie et al., 1997).

The largest class of *Drosophila* learning and memory genes encodes components of the cAMP-dependent signaling pathway (Davis et al., 1995; Davis, 1996; Dubnau and Tully, 1998). Mutants of *dunce*, which encodes a cAMP-specific phosphodiesterase (Byers et al., 1981) and *rutabaga*, which encodes a Ca²⁺/calmodulin- (Ca²⁺/CaM-) dependent adenylyl cyclase (AC) (Levin et al., 1992), have elevated and depressed cAMP levels, respectively, but similarly reduced short-term memory ability (Tully and Quinn, 1985; Tully and Gold, 1993; Davis et al., 1995; Davis, 1996). Studies at the NMJ have revealed several morphological and functional consequences of altered cAMP in these mutants, including altered synaptic terminal morphology (Zhong et al., 1992) and neuronal excitability (Zhong and Wu, 1993; Zhao and Wu, 1997) and impaired activity-dependent synaptic plasticity (Zhong and Wu, 1991). In *Drosophila*, activation of the cAMP-dependent transcription factor CREB (cAMP response element-binding protein) has been shown to underlie long-term memory formation (Yin et al., 1994, 1995) and to regulate functional presynaptic plasticity at the NMJ (Davis et al., 1996). In mammals, cAMP-dependent processes, including CREB activation, are also necessary for long-lasting, transcription-dependent long-term potentiation (LTP) (Frey et al., 1993; Bourtchuladze et al., 1994; Impey et al., 1996; Abel et al., 1997) as well as long-term memory (Bourtchuladze et al., 1994; Goda, 1995a; Abel et al., 1997; Bernabeu et al., 1997). These parallel results underscore the importance of cAMP-dependent mechanisms in regulating highly conserved cellular forms of synaptic plasticity underlying learning and memory.

Screens for *Drosophila* olfactory learning mutants have identified several additional classes of genes with roles in learning and memory. These include *linotte*, encoding a novel protein (Dura et al., 1993; Bolwig et al., 1995); *volado*, encoding an integrin α subunit (Grotewiel et al., 1998); and *leonardo*, encoding a member of the 14-3-3 protein family (Skoulakis and Davis, 1996) involved in regulating multiple types of intracellular signaling (Aitken, 1995). Importantly, all *Drosophila* learning mutants examined to date for synaptic function have significantly altered plasticity properties at the NMJ, consistent with their observed behavioral defects (Zhong and Wu, 1991; Wang et al., 1994; Broadie et al., 1997). For example, *leonardo* was originally identified as a novel learning mutant and subsequently was shown to regulate presynaptic function and modulation properties at the NMJ (Broadie et al., 1997). These findings support the hypothesis that many, if not all, genes involved in learning and memory mechanisms have conserved roles at all synapses, including the NMJ. This

^{||} To whom correspondence should be addressed (e-mail: (broadie@biology.utah.edu).

[#] Present address: University of Pittsburgh School of Medicine, Department of Anesthesiology, Pittsburgh, Pennsylvania 15261.

hypothesis predicts that newly identified mutations affecting learning and memory will have a high likelihood of altering synaptic plasticity properties at the NMJ.

In this study, we have used a genetic approach to study the possible role of a novel learning gene, *latheo* (*lat*), in regulating functional synaptic plasticity. The *lat* gene was identified in a P element mutagenesis screen for *Drosophila* mutants with disrupted 3 hr memory for a Pavlovian olfactory learning task (Boynton and Tully, 1992). The viable P element insertion mutant, *lat^{P1}*, exhibits reduced initial learning ability in olfactory conditioning tests (Boynton and Tully, 1992). Stronger *lat* mutations are lethal in late larval or early pupal stages, indicating the LAT protein has an essential role during larval development as well as a role in adult learning. LAT is a novel synaptic protein with moderate (30% identity) homology to the ORC3 subunit of the human origin replication complex (ORC), and it interacts in vitro with *Drosophila* ORC2, suggesting that LAT functions as part of *Drosophila* ORC (Pinto et al., 1999 [this issue of *Neuron*]). Here, we report that LAT is specifically localized at synaptic boutons of the NMJ, indicating a dual, pioneer synaptic role for this protein. Lethal *lat* mutant alleles exhibit strikingly altered synaptic transmission properties at the NMJ. Evoked transmission is not impaired, but on the contrary, strongly elevated relative to normal. Moreover, mutants exhibit a reduced Ca^{2+} dependence of transmission and strongly impaired activity-dependent synaptic plasticity, including short-term forms of facilitation, longer-term augmentation, and posttetanic potentiation. In these regards, *lat* mutants strongly resemble *dunce* mutants (Zhong and Wu, 1991). LAT's synaptic localization, coupled with the *lat* mutant synaptic phenotype, suggests that the protein may function to modulate synaptic transmission levels during the learning process, possibly through Ca^{2+} - or cAMP-dependent mechanisms.

Results

The LAT Protein Is Present at Synaptic Boutons of the NMJ

A polyclonal antiserum was used to assay LAT protein expression in the larval peripheral nervous system and body muscle. The antiserum is specific for the LAT protein in Western blots of third instar larval CNS extracts, recognizing a single 79 kDa protein from wild-type larvae that is not detectable in *lat^{vr6.6}/lat^{le344}* or *lat³⁴⁴/lat^{le344}* null mutant larvae (data not shown). In wild-type third instar larvae, the LAT protein is immunologically detected at synaptic boutons at most NMJs on a wide variety of muscle fibers in the ventral abdomen (Figures 1B–1F). LAT immunostaining is often only weakly detectable at NMJs containing predominantly large type I boutons, which utilize glutamate as the primary neurotransmitter (Jan and Jan, 1976b; Johansen et al., 1989). Staining is nevertheless clearly evident at type I boutons, including both subtypes Ib and Is (Atwood et al., 1993; Jia et al., 1993), at various NMJs, including muscles 4 and 6/7 (Figures 1B–1D and 1F). At many NMJs, LAT immunostaining is most distinct at morphologically smaller boutons, including those resembling type II and type III boutons (Johansen et al., 1989; Atwood et al., 1993; Jia et

al., 1993) (Figure 1C). These boutons are believed to contain amines and neuropeptides, including octopamine (Monastirioti et al., 1995) and proctolin (Anderson et al., 1988) (type II) and insulin-like peptide (Gorczyca et al., 1993) (type III), which may serve as modulatory transmitters. In particular, the NMJ at muscle 12, which receives types I, II, and III innervation, consistently exhibits positive staining, commonly at multiple bouton types at the same NMJ (Figure 1C). LAT thus appears not to be segregated to particular body segments, subsets of muscle fibers, or particular bouton subtypes distinguishable by morphological or physiological criteria. LAT immunoreactivity is also detectable at the NMJ in second instar larvae (data not shown), indicating the protein is present throughout most of the period of dramatic morphological and functional synaptic maturation.

To gain more specific information on LAT synaptic localization, we carried out double-staining experiments at the wild-type NMJ with antibodies against LAT and other known pre- or postsynaptic proteins. Confocal microscopy of immunofluorescence reveals colocalization of LAT with the presynaptic vesicle-associated cysteine string protein (CSP) (Zinsmaier et al., 1994) at multiple bouton types, including both types I and II (Figure 1E), suggesting LAT is located predominantly presynaptically and colocalizes with synaptic vesicles. LAT and CSP immunostaining often show nearly complete overlap at smaller boutons resembling type II and type III boutons, while at type I boutons, LAT staining usually appears less distinct and contained within a subarea of CSP expression. We also examined LAT localization in preparations double stained for postsynaptic glutamate receptors (DGluR2a; Figure 1D) and the postsynaptic Discs-large (Dlg; Figure 1F) and position-specific β (β PS) integrin proteins (Broadie et al., 1997; data not shown), which are localized in the subsynaptic reticulum of type I boutons. LAT staining typically occupies smaller areas contained within the broader staining pattern of the respective postsynaptic proteins, including the central area of boutons (Figure 1F). These results confirm that LAT is localized at type I boutons and strongly suggest that the protein is expressed predominantly, if not exclusively, in the presynaptic compartment.

Strong *lat* Mutants Are Lethal in Late Larval and Early Pupal Stages

We made detailed morphological and functional examinations of three homozygous lethal *lat* (*lat⁻*) genotypes; two P element excision alleles, *lat^{le49}* and *lat^{le344}*, and an ethyl methanesulfonate- (EMS-) induced allele, *lat^{vr6.6}*, as well as the homozygous viable learning mutant allele *lat^{P1}* (see Experimental Procedures). Homozygous *lat⁻* animals of all three genotypes develop relatively normally through the first and second instars and exhibit coordinated locomotion similar to wild-type larvae. Thereafter, their movement and feeding behavior, though functional, becomes progressively less vigorous. Many mutant larvae grow to normal size but usually remain in the food past the normal wandering stage (5–6 days after egg laying [AEL]) and delay pupation for several days beyond the normal period. Lethality in *lat⁻* larvae and early pupae eventually results from a loss of postembryonic cell division, leading to a complete absence of CNS

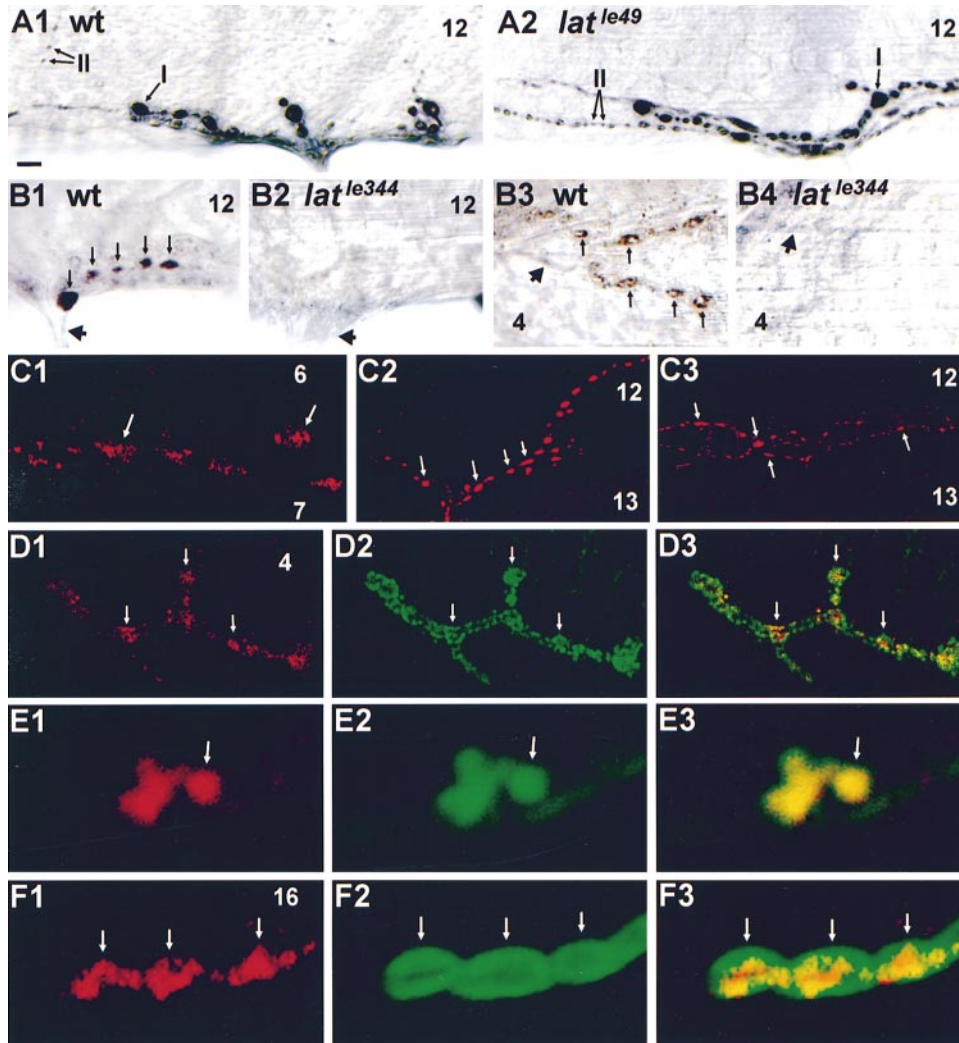


Figure 1. LAT Protein Is Expressed at Larval Neuromuscular Synapses and Enriched at Synaptic Boutons

(A) Wild-type and lethal *lat* mutant NMJs have similar synaptic morphology. Third instar larvae are stained with an antibody against the synaptic vesicle-associated CSP to visualize the presynaptic terminal at muscle 12 in wild-type (A1) and lethal mutant (*lat^{le49}*) (A2) larvae. Type I and type II synaptic boutons are indicated by arrows. Lethal mutant (*lat^{le49}*, *lat^{le344}*) NMJs exhibit normal or mildly altered synaptic morphology compared with wild type (see Figure 2).

(B) LAT protein expression at wild-type NMJs is revealed with an anti-LAT antibody. Examples of LAT protein enriched at individual boutons (indicated by arrows) at the muscle 12 NMJ (B1) and muscle 4 NMJ (B3) of wild-type larvae. Corresponding synaptic fields at muscles 12 (B2) and 4 (B4) in *lat^{le344}* null mutant larvae reveal no detectable protein expression. Large arrowheads indicate the nerve entry point at each NMJ.

(C) LAT is expressed at multiple types of synaptic boutons at a variety of NMJs in wild-type larvae. Panels show confocal images of anti-LAT immunofluorescence at individual NMJs, illustrating presence at type I boutons at muscle 6/7 (C1) and at predominantly smaller boutons (type II and type III) at muscle 12 (C2 and C3).

(D–F) Synaptic colocalization of LAT protein with other pre- and postsynaptic proteins at wild-type larval NMJs.

(D) Confocal images of the same NMJ (muscle 4) double stained with antibodies against LAT (red, [D1]) and postsynaptic DGluR2a (green, [D2]). Several type Ib boutons displaying enriched protein expression are indicated by arrows. The merged image (D3) shows the two protein expression patterns superimposed. LAT synaptic expression at type I boutons is less distinct and is generally confined within a subarea of the DGluR2a postsynaptic expression.

(E) Confocal images at a higher magnification showing a nerve terminal (presynaptic to muscle 12) double stained against LAT (red, [E1]) and CSP (green, [E2]). The arrow indicates one of the several visible synaptic boutons. The merged image (E3) shows the high degree of colocalization of these two proteins, indicated by yellow color, suggesting that LAT is located presynaptically.

(F) Confocal images of the same NMJ (muscle 16) double stained against LAT (red, [F1]) and the postsynaptic Dlg protein (green, [F2]). The merged image (F3) shows LAT synaptic staining at type I boutons occupying a subarea within the postsynaptic Dlg staining, including at the center of boutons, where Dlg staining is weaker.

Scale bar, 10 μ m (A, B, C2, and D); 15 μ m (C3); and 5 μ m (C1, E, and F).

cell proliferation and imaginal development in late third instar (Boynton, 1993; Pinto et al., 1999). All three lethal *lat⁻* alleles appear to be strong protein hypomorphs or

nulls, based on the near or complete absence of detectable LAT protein immunostaining at *lat⁻* NMJs in immunohistological assays (Figure 1B).

Lethal *lat* Mutants Exhibit Only Minor Alterations in Synaptic Morphology

The neuromuscular morphology of *lat*⁻ mutant larvae, including the stereotypic muscle and innervation patterns, appears largely normal. Mutant NMJs are present at the normal synaptic locations and exhibit morphological terminal elaborations, similar to wild-type NMJs. Presynaptic boutons at *lat*⁻ NMJs are normal in size and at the light microscope level appear to possess a normal level of transmitter vesicle proteins, such as CSP (Figure 1A).

Alterations in synaptic terminal morphology have been described for other *Drosophila* learning and memory mutants (Zhong et al., 1992; Wang et al., 1994). We therefore examined the number of terminal branches and synaptic boutons at *lat*^{le49} and *lat*^{le344} NMJs, using anti-CSP to visualize presynaptic terminals (Figures 1A and 2). The terminal branching pattern at the muscle 12 NMJ, which receives multiple innervation and forms boutons of three to four subtypes, is similar to normal for both *lat*^{le49} and *lat*^{le344} larvae (Figure 2A). However, both *lat*⁻ mutant strains have ~20% fewer terminal branches than do wild-type terminals, due to fewer higher order branch segments at mutant terminals (Figure 2B). Consistent with reduced terminal branching, *lat*^{le49} NMJs also have ~20% fewer synaptic boutons than do wild-type NMJs at both muscle 12 and muscle 6/7 (Figure 2C). Similar but statistically insignificant decreases are observed at *lat*^{le344} muscle 12 and 6/7 NMJs, which show more variability in bouton number. However, parallel morphological changes are not observed at the muscle 4 NMJ, where both *lat*^{le49} and *lat*^{le344} NMJs have a statistically insignificant increased bouton number compared to normal (Figure 2C).

In summary, *lat*⁻ mutant NMJs exhibit only mild alterations in synaptic morphology. At the more complex muscle 12 NMJ, mutant terminal complexity appears to be slightly reduced on the basis of terminal branching and bouton number. In contrast, at the simpler muscle 4 NMJ, mutant terminals have normal or slightly increased bouton numbers and terminal complexity. Thus, as we show below, these morphological differences are completely insufficient to account for the functional alterations in transmission at mutant synapses.

Basal Synaptic Transmission Amplitude Is Elevated in *lat* Mutants, but Spontaneous Miniature EJCs Are Not Altered

Synaptic transmission was assayed at *lat* mutant larval NMJs by two electrode voltage-clamp (TEVC) recordings of nerve-evoked excitatory junctional currents (EJCs) at concentrations of external Ca²⁺ ranging from 0.1–1.0 mM. EJC amplitude in the voltage-clamped muscle (–60 mV holding potential) directly reflects the post-synaptic response to presynaptic transmitter release. Recordings were made from muscle 12, which consistently displayed the strongest LAT antibody staining, as well as from muscle 6, which displayed consistently weaker staining.

At a basal stimulation frequency of 0.5 Hz, mutant EJC amplitudes are significantly larger than for wild type at all Ca²⁺ concentrations (Figure 3). In 0.2 mM Ca²⁺, mean EJC amplitude in muscle 12 is about 2-fold larger

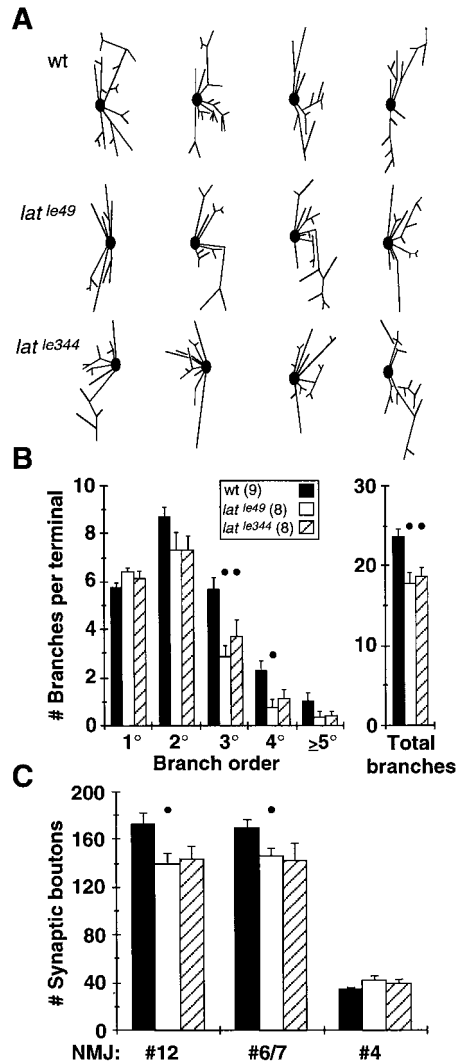


Figure 2. Synaptic Terminal Branching and Bouton Number Are Similar to Normal in Lethal *lat* Mutants

Third instar larvae were fixed and stained with anti-CSP as in Figure 1A to visualize presynaptic terminals at muscles 12, 6/7, and 4 (abdominal segment A2).

(A) Schematic representations of synaptic terminal branching patterns at muscle 12 in wild-type (top row), *lat*^{le49} (middle), and *lat*^{le344} mutant (bottom) larvae; examples from both left and right hemisegments are included. Orientation: anterior, upward; the solid oval represents the nerve entry point.

(B) Summary of synaptic terminal branching at the muscle 12 NMJ for normal and mutant (*lat*^{le49} and *lat*^{le344}) larvae. Both *lat*⁻ mutants have ~20% fewer total terminal branches than wild type at muscle 12 (right panel); this difference is due to an overall reduction in the number of higher order (2°–5°) branches (left panel). Numbers in legend are numbers of larvae analyzed and apply to both (B) and (C). Dots above the bars indicate a statistically significant difference from wild type ($p < 0.05$, two tailed t test).

(C) Synaptic bouton number at wild-type and mutant NMJs. The *lat*^{le49} NMJs have slightly (15%–20%) but significantly fewer boutons at muscles 12 and 6/7 compared with wild type. A similar but insignificant reduction is also observed at *lat*^{le344} NMJs. Neither strain shows a significantly different bouton number compared with wild type at the muscle 4 NMJ.

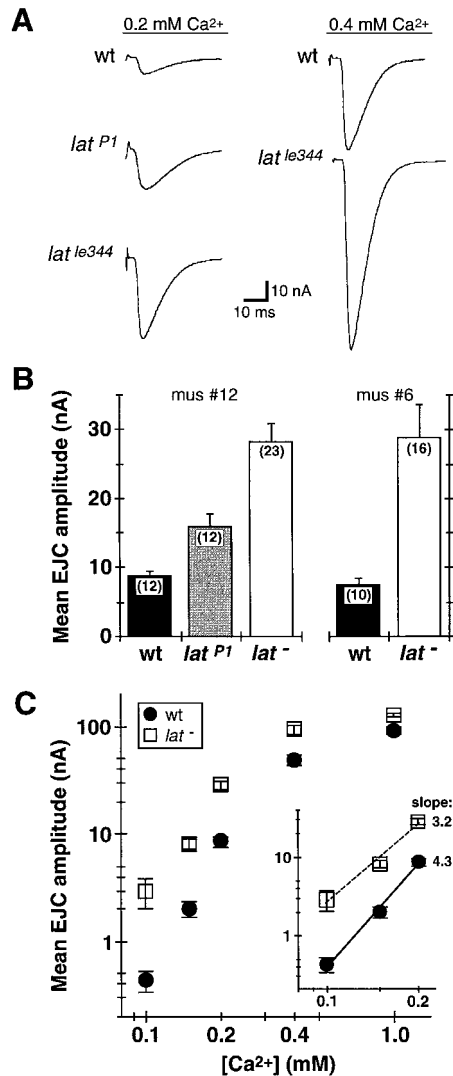


Figure 3. Synaptic Transmission at the Larval NMJ Is Elevated in *lat* Mutants

(A) Representative averaged EJCs evoked in 0.2 mM Ca^{2+} (left) and 0.4 mM Ca^{2+} (right) in wild-type, viable mutant (*lat^{P1}*), and lethal mutant (*lat^{le344}*) larvae. Synaptic transmission was evoked at 0.5 Hz while recording voltage-clamped currents at -60 mV in muscle 12. Each trace is the average of 20 consecutive EJCs.

(B) Mean EJC amplitudes in 0.2 mM Ca^{2+} for muscle 12 (left) and muscle 6 (right) in wild-type (closed bar), *lat^{P1}* (shaded bar), and lethal mutant (*lat⁻*) (open bar) larvae. At both NMJs, *lat⁻* mutant basal EJC amplitude (0.5 Hz stimulation) is over 3-fold larger than for wild type (muscle 12: 28.2 ± 2.7 nA, *lat⁻*, versus 8.6 ± 1.0 nA, wild type; muscle 6: 28.9 ± 4.6 nA, *lat⁻*, versus 7.5 ± 0.9 nA, wild type). No difference in mean EJC amplitude was observed between the three *lat⁻* alleles (*lat^{le49}*, *lat^{le344}*, and *lat^{vr6.0}*). Numbers within the bars indicate the number of larvae analyzed for each group.

(C) Relationship between EJC amplitude and external Ca^{2+} concentration for wild-type and *lat⁻* mutant larvae. Mutant EJC amplitude is elevated relative to wild type over the entire range of external Ca^{2+} concentrations (0.1–1.0 mM). Each point represents mean EJC amplitude (\pm SEM) at basal stimulation frequency (0.5–1.0 Hz) in muscle 12 from at least five larvae. Results from two or three *lat⁻* alleles (open symbols) are pooled at each concentration. Inset plots show the power relationships in the range of 0.1–0.2 mM Ca^{2+} . The lines (fit by regression to each plot) have slopes of 4.3 for wild type (solid line) and 3.2 for *lat⁻* (dotted line).

than normal for the viable learning mutant *lat^{P1}* and 3- to 4-fold larger than normal for the lethal mutants (*lat^{le49}*, *lat^{le344}*, and *lat^{vr6.0}*). No significant differences were observed among the lethal genotypes (pooled as *lat⁻*), which all show the same strong increase in basal transmission amplitude (Figures 3B and 3C). Nearly identical differences between normal and *lat⁻* EJC amplitudes are recorded in muscle 6 (Figure 3B), suggesting the increase in transmission in *lat⁻* mutants is common to all NMJs, despite variability in antibody staining intensity.

The difference between *lat⁻* mutant and wild-type EJC amplitudes decreases with increasing external Ca^{2+} concentrations (Figure 3C), but *lat⁻* transmission remains significantly stronger than normal at 1 mM Ca^{2+} (129 ± 6 nA, *lat⁻*, versus 92 ± 7 nA, wild type). The Ca^{2+} dependence relationship for *lat⁻* transmission over the 0.1–1.0 mM range is shifted significantly to the left, indicating that a lower level of Ca^{2+} is required to achieve a given EJC amplitude (Figure 3C), which accounts for the elevated mutant EJC amplitudes at all Ca^{2+} concentrations tested. In the 0.1–0.2 mM range, both wild-type and *lat⁻* transmission have a linear dependence on external Ca^{2+} in the logarithmic plot, illustrating a power relationship with external Ca^{2+} . However, the slope of the *lat⁻* power relationship (3.2) in this range is significantly less than that for wild type (4.3; Figure 3C). The reduced slope suggests that the Ca^{2+} cooperativity for transmitter release is reduced at mutant NMJs.

To address whether these differences in evoked transmission amplitude and Ca^{2+} dependence result from altered synaptic vesicle exocytosis probability or glutamate receptor field strength, we recorded spontaneous miniature EJCs (mEJCs) in normal and *lat⁻* mutant larvae (*lat^{le49}*, *lat^{le344}*; Figure 4). mEJCs at *lat⁻* NMJs display no significant differences in mean amplitude, variability, spontaneous frequency, or current decay kinetics compared with wild-type mEJCs (Figures 4B and 4C). Normal mEJC amplitude and kinetic properties at the mutant NMJ indicate that postsynaptic glutamate receptor density and channel properties are not significantly altered. The normal mEJC frequency recorded in mutants suggests that the number of active release sites or spontaneous vesicle fusion probability has not been affected. From these results, we conclude that mutations in *lat* appear specifically to alter the Ca^{2+} -dependent, evoked transmission pathway.

Short-Term Synaptic Facilitation Is Strongly Depressed in *lat* Mutants

The *Drosophila* NMJ exhibits multiple forms of functional plasticity similar to those found at central synapses in other systems (Zhong and Wu, 1991; Delgado et al., 1992; Wang et al., 1994; Broadie et al., 1997). Activity-dependent, facilitory forms of synaptic plasticity at the NMJ are most apparent in low external Ca^{2+} conditions (0.1–0.2 mM), at which basal transmission amplitude is reduced (Zhong and Wu, 1991). To assess LAT's role in these synaptic modulation processes, we assayed two forms of short-term synaptic plasticity in 0.2 mM Ca^{2+} , paired-pulse facilitation (PPF) and short-term frequency-dependent facilitation (STF; Figure 5).

Wild-type NMJs exhibit PPF when two consecutive EJCs are evoked at intervals of ≤ 100 ms, with maximal

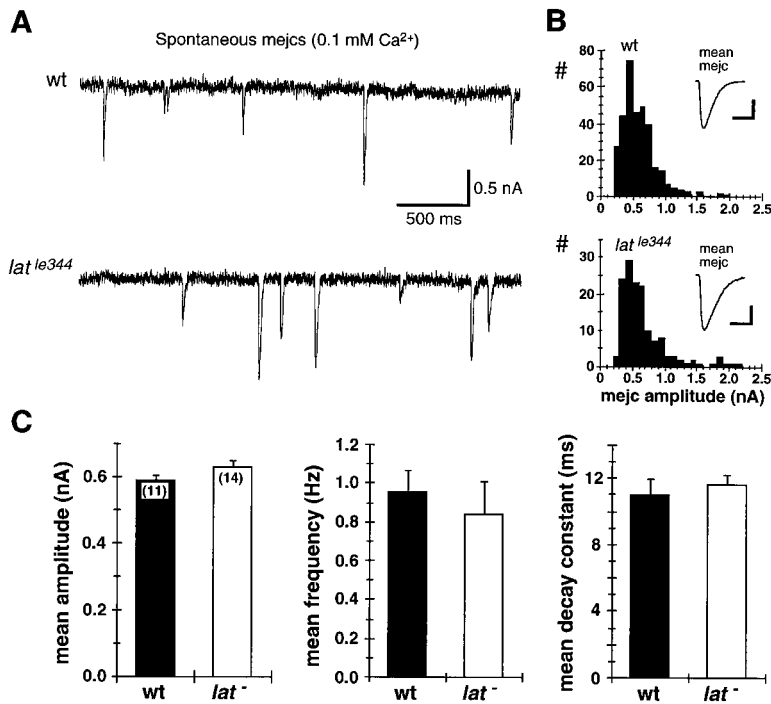


Figure 4. mEJC Amplitude, Frequency, and Decay Kinetics Are Not Significantly Altered in Lethal *lat* Mutants

Spontaneous mEJCs were recorded from muscle 12 (-80 mV, 0.1 mM Ca²⁺) in wild-type and *lat*⁻ mutant (*lat*^{le49} and *lat*^{le344}) larvae.

(A) Sample continuous recordings (3 s) of mEJCs in wild-type and *lat*^{le344} mutant larvae. (B) mEJC amplitude distributions for the recordings shown in (A). The signal-averaged mEJC for each record is shown in inset (mean mEJC); n = 335 events in wild-type (wt) panel and 146 in *lat*^{le344} panel. There is no significant difference overall in mEJC mean amplitude (see below) or variability between wild-type and *lat*⁻ mutant larvae (SD of mEJC amplitude: 0.26 ± 0.02 nA for wild type, n = 11; 0.29 ± 0.02 nA for *lat*⁻, n = 14). Scale bar, 0.2 nA and 30 ms.

(C) Mean mEJC amplitudes (left), frequencies (middle), and decay time constants (right) in wild-type (closed bars) and *lat*⁻ mutant (open bars) larvae. Decay time constants were estimated by fitting a single exponential curve to the averaged mEJC from each recording. No significant difference in these parameters was found between normal and *lat*⁻ mutant larvae. The number of larvae analyzed (n ≥ 7 larvae for each *lat*⁻ genotype) is indicated within the bars in the left panel.

PPF (~2.5-fold) of the second response at 20–30 ms interpulse intervals (Figure 5A). As described above, initial EJC amplitude is strongly elevated in *lat*⁻ mutants, as though transmission is in a “prefacilitated” state. Further PPF is strongly reduced for all *lat*⁻ genotypes and is sometimes replaced by depression at shorter intervals. At 20–30 ms interpulse intervals, average PPF at *lat*⁻ NMJs is reduced to ~20% of wild-type level. The viable *lat*^{P1} mutant, which has an intermediate initial transmission amplitude, exhibits a stronger PPF of ~75% of wild-type level (Figure 5A).

When normal NMJs are stimulated with short trains at 2–20 Hz, EJC amplitude undergoes facilitation during the train in a frequency-dependent manner (STF; Figure 5B). Facilitation of 3- to 4-fold occurs for 20 Hz stimulation and is short-lived in all cases, returning to initial amplitude after several seconds rest. At *lat*⁻ NMJs, STF is greatly reduced over the entire range of stimulation frequencies and does not differ significantly overall among the three lethal genotypes (*lat*⁻; Figure 5B). At higher stimulation frequencies (10–20 Hz), responses among individual *lat*⁻ larvae vary from mild facilitation to mild depression, with average STF reduced to ~30% of normal. The viable *lat*^{P1} mutant exhibits stronger facilitation of ~80% of wild-type level (Figure 5B). Thus, *lat* mutant NMJs show reduced plasticity for each of these short-lived forms of facilitation. These defects are comparatively mild but significant for the viable learning mutant *lat*^{P1}; however, *lat*⁻ mutant NMJs have severely compromised ability for short-term facilitation.

Synaptic Augmentation and Posttetanic Potentiation Are Strongly Impaired in *lat* Mutants

During prolonged (>30 s) tetanic stimulations at moderate frequencies (5–10 Hz), the *Drosophila* NMJ displays significant augmentation of synaptic transmission as

well as posttetanic potentiation (PTP) following the stimulus train (Zhong and Wu, 1991). To assay these longer-term forms of synaptic modulation in *lat* mutants, the NMJ was stimulated in 0.2 mM Ca²⁺ at an initial basal frequency (0.5 Hz) for 30 s followed by a 60 s stimulation at 5 Hz. PTP was measured for several minutes at 0.5 Hz following the tetanus (Figure 6A). Under these stimulation conditions, normal NMJs rapidly undergo facilitation followed by a gradual and maintained augmentation of EJC amplitude, reaching 2- to 2.5-fold over initial control levels at the end of the tetanus. Robust initial PTP of 2-fold or greater over initial control amplitude persists for >1 min after the tetanus followed by a gradual decline (Figure 6B). Average PTP at wild-type NMJs remains significant (25%–50%) at the end of a 3.5 min posttetanus period, resulting in a prolonged potentiation of basal transmission amplitude.

All of the *lat* mutant alleles display strongly impaired synaptic augmentation and PTP (Figure 6B). The viable *lat*^{P1} mutant, consistent with its comparatively mild defects in STF, exhibits essentially a weakened version of wild-type augmentation and PTP. Initial facilitation and weak-to-moderate augmentation to ~75% over control amplitude occur during the tetanus followed by initial PTP 40%–50% of normal strength, which decays gradually to near initial control amplitude. The *lat*^{P1} allele thus shows moderate but significant depression of longer-term as well as short-term synaptic enhancement. For the lethal alleles *lat*^{le49} and *lat*^{vr6.6}, augmentation is completely absent and is sometimes replaced by depression, and posttetanus EJC amplitudes show only extremely weak (~20%) PTP for 30–60 s. The *lat*^{le344} larvae display mild augmentation and initial (~30 s) PTP more similar to *lat*^{P1} larvae; thereafter, however, PTP is indistinguishable from the other lethal alleles (Figure 6B). The maintained, longer-term component of PTP is completely absent at *lat*⁻ mutant NMJs. These physiological

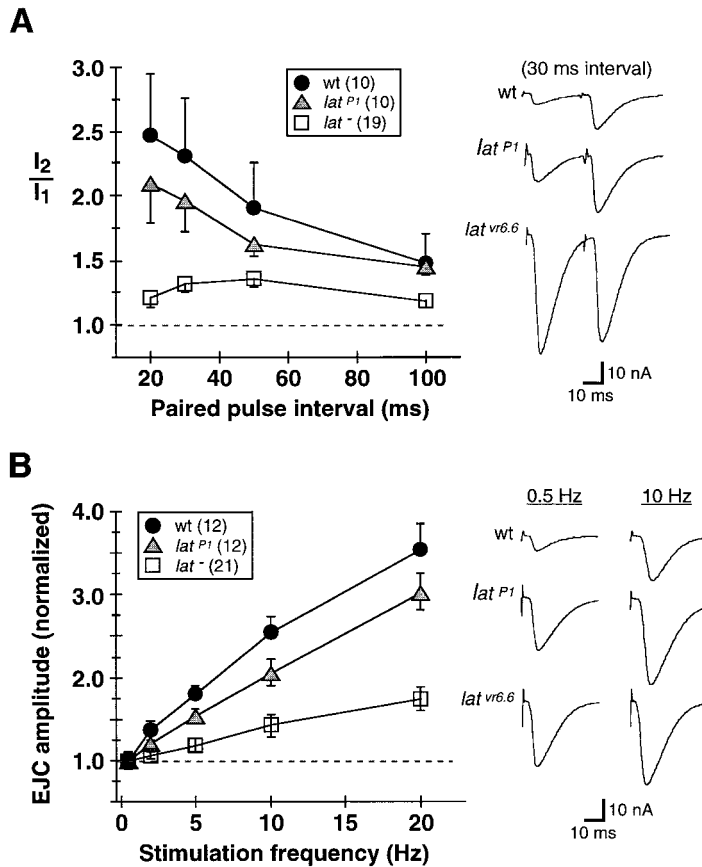


Figure 5. PPF and STF Are Strongly Impaired in Lethal *lat* Mutants

The ability of mutant NMJs to display these two short-term forms of facilitation was assayed in 0.2 mM Ca²⁺.

(A) Mutant PPF. Responses to five to ten consecutive paired stimuli (separated by 4 s rest) at 20–100 ms interpulse intervals were averaged. Traces show representative averaged responses at 30 ms interstimulus interval for wild-type, viable mutant (*lat*^{P1}), and lethal *lat*⁻ (*lat*^{vr6.6}) mutant larvae. At 20–30 ms intervals, wild-type NMJs exhibit ~2.5-fold PPF, while *lat*⁻ mutant NMJs exhibit only weak PPF or even depression (*lat*^{vr6.6}, lower trace). Plot summarizes PPF for wild-type and mutant larvae. Facilitation (I₂/I₁) is expressed as the mean amplitude ratio of response 2 to response 1 at each interval. The *lat*⁻ mutants show strongly reduced PPF at all intervals <100 ms. No significant differences in PPF were observed among the three *lat*⁻ mutant genotypes (*lat*^{le49}, *lat*^{le344}, and *lat*^{vr6.6}).

(B) Mutant STF. Trains of 20 stimuli were delivered to the NMJ at 0.5–20 Hz frequencies. The amplitudes of the last ten responses in each train were averaged and normalized to the average amplitude at 0.5 Hz as an assay of frequency-dependent STF (Zhong and Wu, 1991). Traces show averaged EJCs (last 10 of 20 responses) for 0.5 Hz and 10 Hz trains for wild-type, viable *lat*^{P1} mutant, and *lat*⁻ mutant (*lat*^{vr6.6}) larvae. Wild-type NMJs exhibit ~2.5-fold facilitation at 10 Hz stimulation. In *lat*⁻ mutants, initial transmission at 0.5 Hz is strongly elevated relative to normal (see Figure 3) and shows on average only weak facilitation.

Plot summarizes STF (normalized to EJC amplitude at 0.5 Hz) for wild-type and mutant larvae. STF is ~80% of wild-type level for *lat*^{P1} larvae but is strongly depressed for *lat*⁻ mutants at frequencies ≥2 Hz. No significant differences were observed among the three *lat*⁻ mutant genotypes.

results are in agreement with adult *Drosophila* behavioral assays, in which viable heteroallelic *lat*^{P1}/*lat*⁻ combinations exhibit more severe deficits in olfactory associative learning than *lat*^{P1} homozygotes (Boynton and Tully, 1992). All of the lethal *lat* alleles therefore display severe defects in both longer-term and short-term synaptic plasticity, results consistent with the *lat* gene's involvement in adult learning.

Mutant Synaptic Plasticity Defects Are Not Eliminated by Reducing Basal Transmitter Release

One model for the *lat* mutant synaptic phenotype suggested by the above results is that *lat*⁻ mutant transmission is already strongly or maximally facilitated in the low-Ca²⁺ condition (0.2 mM) used to assay activity-dependent facilitation. In support of this model, basal EJC amplitude recorded in *lat*⁻ larvae in 0.2 mM Ca²⁺ (28.2 ± 2.7 nA, 0.5 Hz stimulation) is elevated to the amplitude of strongly facilitated wild-type EJCs (28.5 ± 2.6 nA, 20 Hz stimulation). High-frequency stimulation produces further facilitation of no more than 25%–50%, suggesting that the mutant transmission machinery may already be working at near maximum capacity. Such a defect could result from a Ca²⁺ dependence relationship that is effectively shifted to the left, toward lower [Ca²⁺] (Figure 3C). If so, the effect of such a shift should be

reversible by further reducing external Ca²⁺ to reduce *lat*⁻ basal EJC amplitude to a normal level.

We tested this idea by reexamining synaptic plasticity parameters of both *lat*⁻ mutant and wild-type NMJs in further reduced external Ca²⁺. As shown in Figure 7A, *lat*⁻ basal EJC amplitude (0.5 Hz stimulation) in 0.15 mM Ca²⁺ is identical to wild-type EJC amplitude in 0.2 mM Ca²⁺, suggesting that *lat*⁻ and wild-type transmission properties are comparable under these two conditions. Consistent with the above hypothesis, *lat*⁻ NMJs in 0.15 mM Ca²⁺ show stronger frequency-dependent STF for 5–20 Hz stimuli (Figures 7B–7D). However, *lat*⁻ STF over the entire frequency range remains significantly weaker than for wild type in 0.2 mM Ca²⁺, and much weaker when compared directly to wild-type STF in 0.15 mM Ca²⁺ (Figure 7D). Overall, *lat*⁻ mutant STF in 0.15 mM Ca²⁺ is “rescued” only to near the level recorded from *lat*^{P1} mutant larvae in 0.2 mM Ca²⁺ (compare with Figure 5D). In 0.15 mM Ca²⁺, PPF is decreased for wild-type and slightly improved for *lat*⁻ NMJs compared with that in 0.2 mM. However, *lat*⁻ mutant PPF remains severely depressed compared with the wild-type level in 0.2 mM Ca²⁺ (Figure 7C). Thus, even when basal transmission output is equalized, these forms of short-term modulation are only partially restored in *lat*⁻ mutants. These results suggest that *lat* mutants show specific defects in short-term Ca²⁺-dependent synaptic modulation that

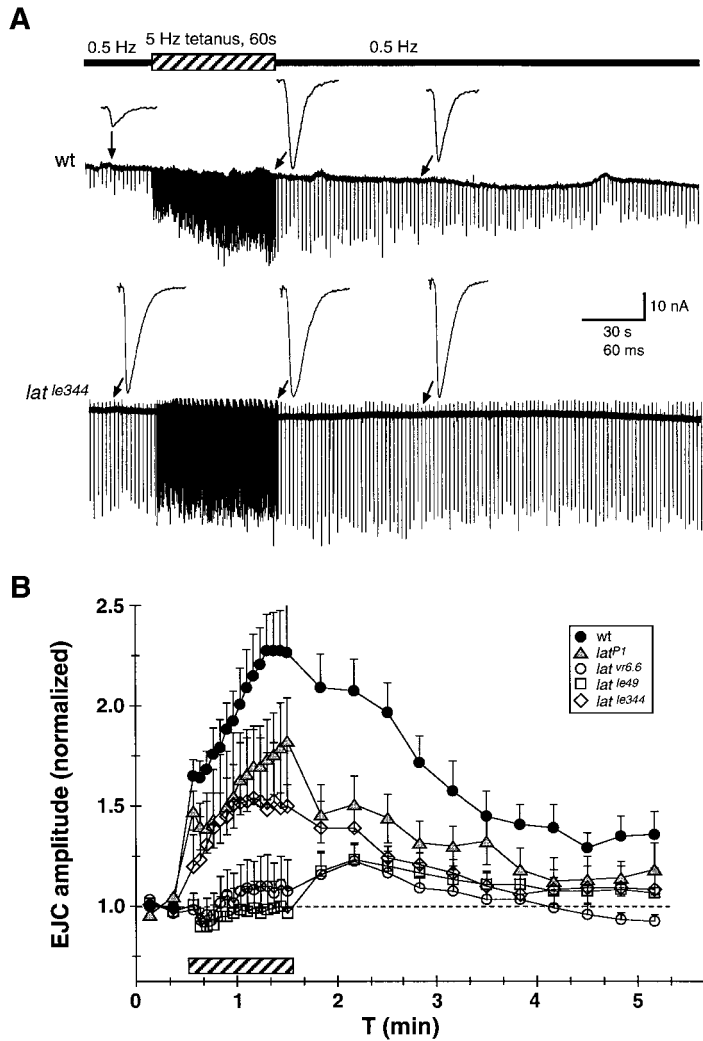


Figure 6. Synaptic Augmentation and PTP Are Strongly Impaired in *lat* Mutants

These longer-term plasticity properties were examined in 0.2 mM Ca^{2+} .

(A) Example continuous records from wild-type and lethal mutant (*lat^{le344}*) larvae. The first 200 s of a 300 s record are shown in each trace. Initial control EJCs were recorded at 0.5 Hz stimulation for 30 s followed by 5 Hz stimulation for 60 s (indicated by hatched bar). PTP was measured for a period of 3.5 min after returning to the initial 0.5 Hz stimulation frequency. Individual EJCs shown in expanded time scale above each trace (arrows) were recorded during the initial control period, near the end of the tetanus, and ~70 s following the end of the tetanus. Scale bar, 10 nA and 30 s (continuous traces) or 60 ms (inset traces).

(B) Summary of PTP in wild-type and *lat* mutant larvae. Each plot represents mean (\pm SEM) for 5–12 fibers from each genotype. For each experiment, EJC amplitude was normalized to the initial mean amplitude at 0.5 Hz. Normalized amplitudes were then averaged for each 20 consecutive EJCs during the tetanus period and for each 10 consecutive EJCs during the posttetanus period. Wild-type NMJs (closed circles) exhibit rapid initial facilitation followed by a gradual augmentation of EJC amplitude for most of the tetanus period. Initial PTP is greater than 2-fold over control amplitude and gradually declines thereafter but on average remains significantly elevated (25%–30%) after 3.5 min. The lethal *lat* mutants (open symbols) exhibit varying defects compared with wild type. For *lat^{le49}* and *lat^{vr6.6}* alleles, augmentation is in some cases replaced by depression during the tetanus, and only weak, short-lived PTP (~20% over initial amplitude) is observed. The *lat^{le344}* allele exhibits stronger tetanic augmentation on average but only weak initial PTP (~30% over initial amplitude) for ~1 min. The viable *lat^{P1}* allele (shaded symbols) shows moderate augmentation and sustained PTP, but both at levels substantially weaker than normal.

are not simply the result of elevated or saturated basal transmission.

In 0.15 mM Ca^{2+} , all three *lat* genotypes display improved synaptic augmentation during prolonged (60 s) 5 Hz stimulation (Figure 7E). The relative levels of augmentation observed for each mutant allele are consistent with the severity of phenotype observed above in 0.2 mM Ca^{2+} (compare with Figure 6B). The *lat^{le344}* larvae show the strongest average augmentation, to levels 80%–90% that of normal larvae in 0.2 mM Ca^{2+} (Figure 7E). Progressively weaker augmentation occurs for *lat^{vr6.6}* and *lat^{le49}* larvae, respectively. Thus, although each genotype shows partial rescue of the augmentation defect, augmentation remains significantly depressed overall compared with normal, and dramatically poorer when compared directly with normal, in 0.15 mM Ca^{2+} . Moreover, for each *lat* genotype, the augmented EJC amplitude cannot be sustained and declines within seconds following the tetanus. The mutant NMJs show no

improvement in the minimal (~20%), short-lived PTP observed in 0.2 mM Ca^{2+} (Figures 6B and 7E), with the exception of *lat^{le49}* larvae, which exhibit severely reduced (25%–30%) PTP for several minutes. In contrast, wild-type PTP is prolonged further in 0.15 mM Ca^{2+} than that observed in 0.2 mM. The ability to develop and maintain increased transmission therefore remains strongly impaired in *lat* mutants when compared with that of wild type at the same Ca^{2+} level and at external Ca^{2+} , at which normal and mutant synaptic output is equal.

Transgenic Expression of the *lat* Gene in Null Mutants Rescues Synaptic Transmission and Plasticity Defects

As further support for the hypothesis that LAT has a specific role in synaptic function, we examined synaptic transmission in null mutant (*lat^{le344}*) animals with a stable

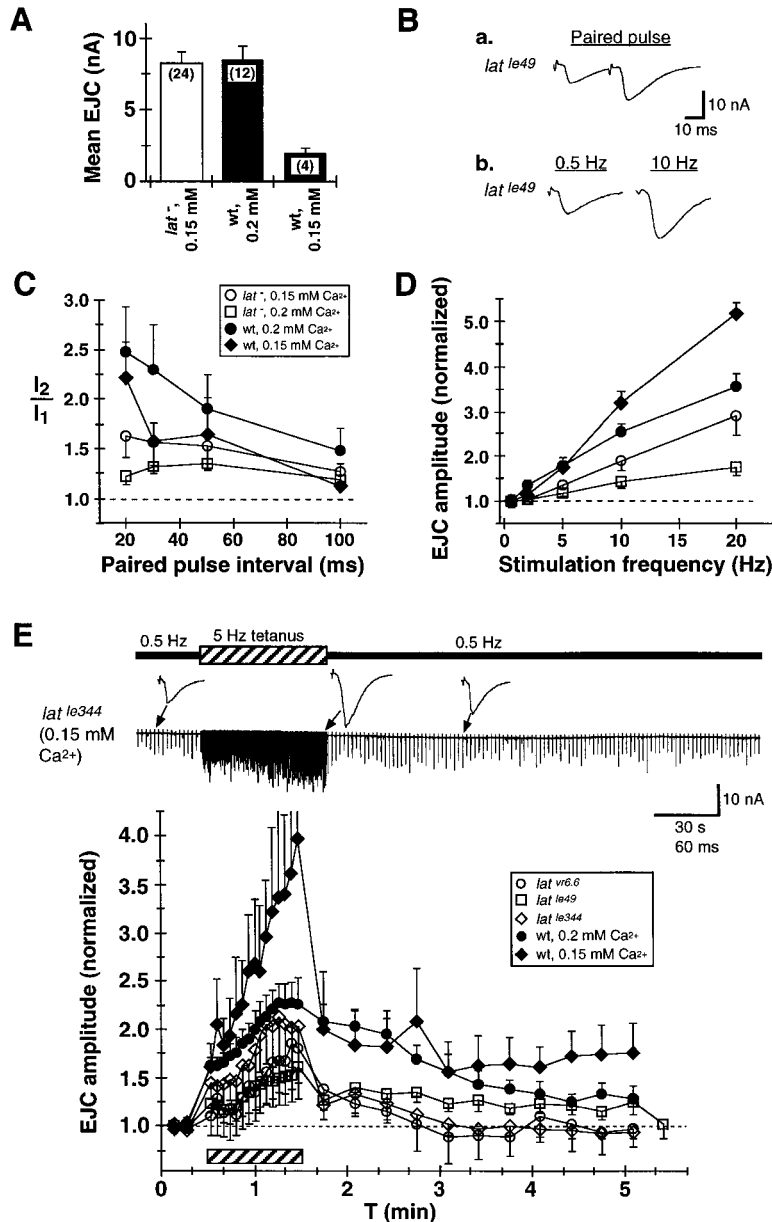


Figure 7. Synaptic Plasticity Deficits in Lethal *lat* Mutants Are Incompletely Restored by Reducing Basal Transmitter Release

Short-term forms of facilitation (PPF, STF), synaptic augmentation, and PTP parameters were examined as in Figures 5 and 6 in *lat*⁻ and wild-type larvae in reduced (0.15 mM) external Ca²⁺.

(A) Mean EJC mean amplitude (0.5 Hz stimulation) in 0.15 mM Ca²⁺ for lethal *lat*⁻ mutant genotypes (left bar) is indistinguishable from wild-type EJC amplitude in 0.2 mM Ca²⁺ (middle bar), demonstrating that mutant and normal basal synaptic output levels are equal under these respective conditions. No significant differences in mean transmission amplitude were observed among the three *lat*⁻ genotypes (*lat*^{le49}, *lat*^{le344}, and *lat*^{vr6.6}; n ≥ 4 larvae for each genotype). By comparison, in 0.15 mM Ca²⁺, wild-type EJC amplitude (right bar) is substantially reduced compared with *lat*⁻. (B) Representative averaged EJCs in 0.15 mM Ca²⁺ for a *lat*^{le49} larva showing responses to paired-pulse stimulations (30 ms interval, [Ba]) and to 0.5 Hz and 10 Hz stimuli (Bb) in 0.15 mM Ca²⁺.

(C) Summary of wild-type and *lat*⁻ mutant PPF in 0.15–0.2 mM Ca²⁺. PPF in *lat*⁻ mutants shows only slight improvement in 0.15 mM (open circles) compared with 0.2 mM Ca²⁺ (squares) and remains substantially weaker than wild-type PPF in 0.2 mM Ca²⁺ (closed circles). Wild-type PPF is also reduced in 0.15 mM Ca²⁺ except for the briefest (20 ms) interpulse interval.

(D) Summary of wild-type and *lat*⁻ mutant STF in 0.15–0.2 mM Ca²⁺. STF in *lat*⁻ mutants is substantially stronger in 0.15 mM than in 0.2 mM Ca²⁺, but it is still weaker than wild-type STF in 0.2 mM Ca²⁺ and is much weaker than wild type in 0.15 mM Ca²⁺.

(E) Summary of wild-type and *lat*⁻ mutant PTP in 0.15–0.2 mM Ca²⁺. Upper panel, continuous recording from a *lat*^{le344} larva in 0.15 mM Ca²⁺. The first 200 s of a 300 s record are shown. Individual EJCs shown above the continuous trace (arrows) were recorded during the initial control period (0.5 Hz), near the end of the tetanus (60 s at 5 Hz) period and ~60 s following the end of the tetanus. The mutant NMJ shown exhibits initial facilitation

followed by augmentation for the duration of the tetanus and moderate (~50%) PTP for about 1 min following the tetanus. Scale bar, 10 nA, 30 s (continuous traces) and 60 ms (inset traces).

Lower panel, open symbols show averaged normalized responses (±SEM) from greater than or equal to four fibers of each *lat*⁻ genotype. Closed symbols show wild-type PTP in 0.15 mM (diamonds) and 0.2 mM (circles) Ca²⁺. In 0.15 mM Ca²⁺, wild-type augmentation is much stronger than that observed in 0.2 mM, initial PTP following the tetanus is unchanged, and later PTP (4–5 min) is slightly increased. Among *lat*⁻ mutant strains (open symbols), synaptic augmentation during the tetanus is strengthened in 0.15 mM Ca²⁺ compared with that observed in 0.2 mM Ca²⁺ (compare with Figure 6), particularly for *lat*^{le344}. Mutant augmentation remains weaker than for wild type in 0.2 mM Ca²⁺, however, and much weaker than wild type in 0.15 mM Ca²⁺. Mutant PTP in 0.15 mM Ca²⁺ is not significantly increased compared with that observed in 0.2 mM Ca²⁺ except for *lat*^{le49}, which show weak (25%–30%) maintained PTP. For all the *lat*⁻ mutants, PTP in 0.15 mM Ca²⁺ remains significantly weaker than for wild type in 0.2 mM Ca²⁺.

transgenic insertion of the wild-type *lat* genomic transcript, *glat*³⁻¹, on the third chromosome (*lat*^{le344}/*lat*^{le344}; *glat*³⁻¹/*glat*³⁻¹). The transgenic construct fully rescues the null mutant lethality and restores normal adult olfactory learning (Pinto et al., 1999). Consistent with the rescue of viability and learning deficits, *lat*^{le344}; *glat*³⁻¹/*glat*³⁻¹ NMJs have EJC amplitudes in 0.2 mM Ca²⁺ that are indistinguishable from those of wild type (Figure 8A),

indicating complete rescue of the *lat*⁻ elevated EJC phenotype. Likewise, both PPF and frequency-dependent STF in *glat*³⁻¹ larvae are rescued to levels comparable to or greater than those observed for wild type (Figures 8B–8D). In particular, STF produced by repetitive high-frequency stimuli (10–20 Hz) is significantly enhanced over normal level (Figure 8D). Similarly, during prolonged tetanic stimulation (60 s at 5 Hz), *glat*³⁻¹ NMJs dis-

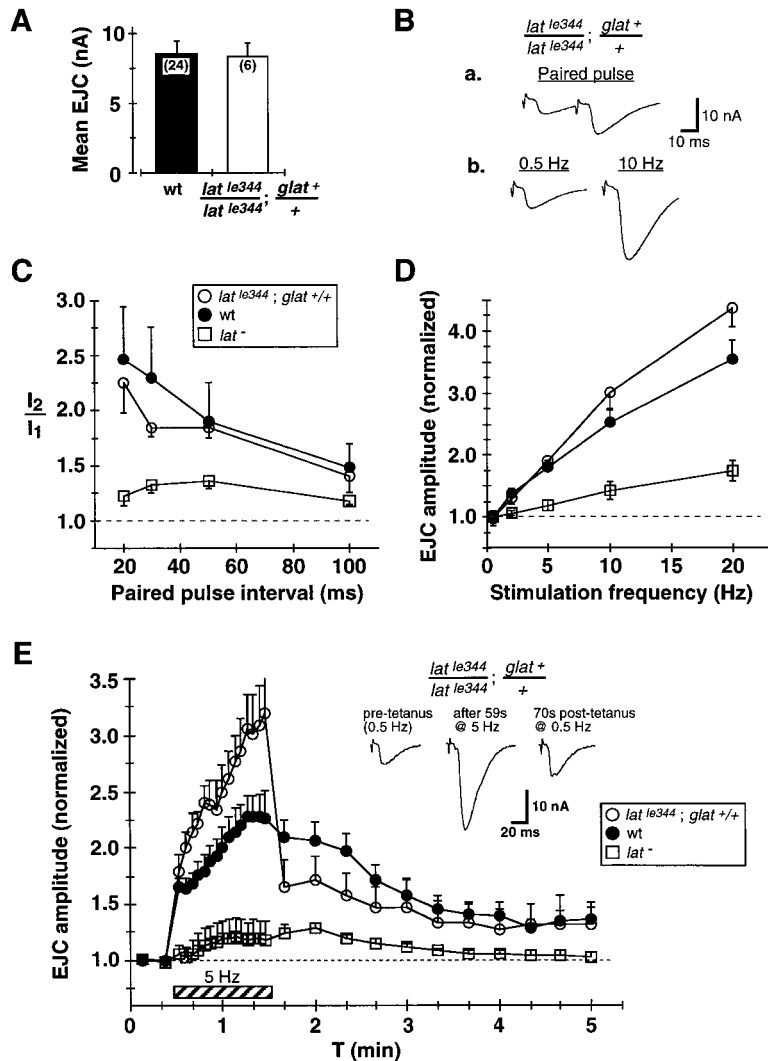


Figure 8. Rescue of *lat* Mutant Transmission Amplitude and Plasticity Defects by *lat*⁺ Transgene

Synaptic transmission properties in 0.2 mM Ca²⁺ were examined as in Figures 5 and 6 in null mutant larvae with a transgenic insertion of the *glat*⁺ *lat* genomic transcript (*lat*^{le344}/*lat*^{le344}; *glat*⁺/+).

(A) The *glat*⁺ 3-1 rescue construct restores mutant basal transmission amplitude (0.5 Hz stimulation) to normal level.

(B) Representative averaged EJCs for a *glat*⁺ 3-1 larva showing PPF ([Ba], 30 ms interval) and responses to 0.5 Hz and 10 Hz stimuli (Bb).

(C and D) Summary of PPF (C) and frequency-dependent STF (D) in *glat*⁺ 3-1 rescue larvae (open circles). Wild-type (closed circles) and *lat*⁻ mutant (squares) plots in 0.2 mM Ca²⁺ are included for comparison. The *glat*⁺ 3-1 PPF shows nearly complete rescue, while STF at higher frequencies (10–20 Hz) is rescued to significantly greater than normal level.

(E) Summary of synaptic augmentation and PTP in *glat*⁺ 3-1 larvae; wild-type and *lat*⁻ mutant plots in 0.2 mM Ca²⁺ are included for comparison. Synaptic augmentation during tetanic stimulation (60 s at 5 Hz, indicated by hatched bar) is significantly enhanced over normal levels in *glat*⁺ 3-1 larvae. PTP is rescued to ~60% of normal level in the first minute following the tetanus and is completely rescued after the first minute to the level (~30% over control pretetanus amplitude) seen in wild type. Inset traces show individual EJCs recorded from a *glat*⁺ 3-1 larva during the control pretetanus period (0.5 Hz stimulation, left trace), after 59 s stimulation at 5 Hz (middle trace), and 70 s following the end of the tetanus (0.5 Hz, right trace).

play markedly enhanced synaptic augmentation ~50% greater than normal (Figure 8E). Finally, the *glat*⁺ 3-1 construct significantly rescues the mutant PTP deficit. In the initial minute, *glat*⁺ 3-1 PTP is improved to ~60% of the normal level, but thereafter, PTP in *glat*⁺ 3-1 and wild-type larvae is indistinguishable (Figure 8E). Thus, transgenic rescue of LAT expression in null mutants restores normal transmission strength and restores all forms of plasticity analyzed to strengths that approach or exceed normal levels. We therefore conclude that LAT functions both to determine or regulate the level of basal transmission and to regulate both short-term and long-term Ca²⁺-dependent synaptic modulation mechanisms.

Discussion

This study demonstrates a synaptic function for a novel learning gene identified through a forward genetic approach in *Drosophila* (Boynton and Tully, 1992), in contrast to previous studies that have focused exclusively on synaptic components first identified in other systems. The LAT protein shares moderate amino acid sequence

homology (30% identical, 42% similar) to a recently identified human ORC subunit, ORC3 (Pinto et al., 1999). LAT coimmunoprecipitates with DmORC2, and null *lat* mutations disrupt imaginal development and CNS proliferation, indicating that LAT functions in cell division as part of *Drosophila* ORC. However, LAT is also expressed cytoplasmically in adult CNS (Pinto et al., 1999), suggesting additional functions in terminally differentiated neurons.

We have shown that LAT is localized to neuronal synaptic boutons and regulates both evoked transmission amplitude and activity-dependent forms of synaptic facilitation and potentiation. Functional synaptic defects in *lat* mutants are strikingly similar to those in the cAMP mutant *dunce*. However, *lat* mutations produce far less distinctive alterations in NMJ synaptic morphology than those observed for *dunce* (Zhong et al., 1992) and thus specifically affect functional aspects of synaptic transmission and plasticity. Based on our results, LAT appears to have two roles in the presynaptic terminal, independent from a possible function in DNA replication: (1) regulation of Ca²⁺-dependent, basal-evoked transmission, including the Ca²⁺ sensitivity of release, and

(2) regulation of both short- and longer-term aspects of Ca^{2+} - and/or cAMP-dependent synaptic modulation. We suggest that LAT may serve similar functions at central synapses involved in learning in the adult brain.

LAT Is Expressed at Synaptic Boutons of the NMJ

We have assayed LAT synaptic function at the accessible neuromuscular synapse. LAT protein is enriched at synaptic connections at the time that robust synaptic plasticity properties develop and mature, consistent with a role for the protein in modulating synaptic function. The variability in LAT antibody staining we observe at different synapses may reflect an uneven or dynamic peripheral expression pattern for the protein or, alternatively, variability in the effectiveness of the antibody staining. While we cannot rule out the latter possibility, it is nevertheless clear the protein is expressed at all morphological subtypes of boutons at the NMJ, including those primarily utilized for fast glutamatergic transmission (Jan and Jan, 1976a, 1976b; Johansen et al., 1989) (type I) as well as those that may have modulatory or regulatory functions (Keshishian et al., 1993) (types II and III). LAT is distinctively colocalized at synaptic boutons with the presynaptic vesicle protein CSP. Colabeling experiments with markers for postsynaptic proteins, including DGluR2a, Dlg, and β PS integrin, also suggest that the LAT protein is restricted to the presynaptic compartment. These results are consistent with our findings that presynaptic plasticity mechanisms are defective in *lat* mutants. We propose that LAT is presynaptically located on the basis of these results but cannot presently exclude the possibility of its presence postsynaptically.

LAT Regulates Synaptic Transmission Amplitude and Short-Term Synaptic Facilitation at the NMJ: Possible Role in Presynaptic Ca^{2+} Regulation

Mutant *lat* NMJs exhibit strongly elevated basal-evoked synaptic transmission over a wide range of external Ca^{2+} concentrations. EJC amplitude in lethal *lat*⁻ mutants is three to four times larger than normal in low Ca^{2+} at both the muscle 12 and 6 NMJs, suggesting that LAT likely has a similar function at all NMJs. However, these NMJs in *lat*⁻ mutants exhibit no significant morphological alterations that can be correlated with increased transmission strength, such as greater numbers of terminal branches or synaptic boutons (Zhong et al., 1992; Wang et al., 1994). The muscle 12 NMJ is, by contrast, slightly simplified in *lat*⁻ larvae compared to normal, forming fewer higher-order branches and synaptic boutons. Removal of the protein in *lat*⁻ mutants thus has primarily a functional consequence on the regulation of presynaptic transmitter release. Furthermore, we observe normal mEJC amplitude and frequency for *lat*⁻ mutants, indicating that neither postsynaptic glutamate receptor density nor the rate of spontaneous presynaptic vesicle exocytosis, respectively, appear to be altered. The increased evoked mutant transmission is thus presynaptically mediated and specific to the Ca^{2+} -dependent, evoked release pathway.

Though *lat* mutants have enhanced, prefacilitated basal-evoked release, the ability of mutant synapses to

undergo further activity-dependent increase in transmission appears to be severely defective. Under low- Ca^{2+} conditions (0.2 mM) that ordinarily favor Ca^{2+} - and activity-dependent forms of synaptic facilitation, *lat* mutants have strongly depressed PPF and frequency-dependent STF. These forms of facilitation common to most synapses are generally believed to reflect enhanced transmitter release due to transient, residual increases in presynaptic Ca^{2+} during repetitive high-frequency stimulation (Zucker, 1993; Fischer et al., 1997). These short-term plasticity defects in *lat*⁻ mutants do not appear to result simply from already saturated Ca^{2+} -dependent plasticity mechanisms. When we further reduce external Ca^{2+} to enhance short-term activity-dependent increases in presynaptic Ca^{2+} , *lat*⁻ mutant PPF and STF are incompletely restored even though basal EJC amplitude is equal to normal.

The regulation of transmitter release by intracellular Ca^{2+} has been examined at various synapses using a combination of techniques (Zucker, 1993, 1996; Kamiya and Zucker, 1994; Fischer et al., 1997). Evoked, prefacilitated exocytosis is triggered by extremely rapid Ca^{2+} influx and binding to fast, low-affinity molecular targets directly at the active site. Short-term facilitation (lasting 1 ms to 1 s) as well as augmentation and PTP (lasting seconds to minutes) are thought to be due to the continuing action of Ca^{2+} at distinct domains in the presynaptic terminal, each with different affinities for Ca^{2+} (Zucker, 1993, 1996; Fischer et al., 1997). Rapid forms of facilitation, including PPF and STF, appear to result from residual Ca^{2+} binding to sites at or near the site of rapid exocytosis. More prolonged forms of facilitation, including augmentation and PTP, may be induced by longer-lived, lower levels of residual Ca^{2+} acting at different sites in the terminal (Zucker, 1996).

Our results suggest that one possible functional role for LAT may be in regulating Ca^{2+} levels or dynamics at one or more of these putative presynaptic domains. The LAT protein appears to be localized in the same proximity as synaptic vesicles. The elevated level of evoked transmitter release, shift in Ca^{2+} dependence, and reduced Ca^{2+} cooperativity of release at *lat*⁻ NMJs suggest that the protein may regulate Ca^{2+} concentration or binding affinity at the rapid release site. However, the loss of short-term facilitation, augmentation, and PTP (see below) in *lat*⁻ mutants suggests the release dependence is also altered at other presynaptic Ca^{2+} domains involved in mediating these forms of plasticity. It is difficult to propose a Ca^{2+} regulatory scheme that can account for this combination of *lat* transmission defects. The increased mutant transmission phenotype could be produced by increased basal levels of presynaptic Ca^{2+} resulting from alterations in presynaptic Ca^{2+} sequestration or buffering. For example, presynaptic reticulum (Fossier et al., 1993, 1998) and mitochondrial Ca^{2+} stores (Alnaes and Rahamimoff, 1975; Tang and Zucker, 1997; David et al., 1998) have been proposed to play important roles in presynaptic Ca^{2+} sequestration at other synapses and can regulate both basal Ca^{2+} level and transmitter release as well as Ca^{2+} -dependent synaptic plasticity. However, other aspects of *lat* mutant transmission are at odds with a generalized role in Ca^{2+} regulation. Most significantly, we observe no increase in *lat*⁻ mutant mEJC frequency, as would be expected

from increased basal presynaptic Ca^{2+} levels resulting from a mitochondrial or Ca^{2+} buffering defect (Alnaes and Rahamimoff, 1975). Second, whereas inhibiting presynaptic Ca^{2+} sequestration increases facilitation at *Aplysia* synapses (Fossier et al., 1993, 1998), synaptic facilitation in *lat* mutants is absent or depressed even at low external Ca^{2+} . Further work will be necessary to determine how LAT may be involved in presynaptic Ca^{2+} action at various domains following Ca^{2+} influx as well as during activity-dependent synaptic facilitation.

LAT May Have a Role in cAMP-Dependent Forms of Synaptic Modulation: Relation to *Drosophila* cAMP Mutants

Lethal *lat* mutants display strongly impaired synaptic augmentation during prolonged tetanic stimulation and severely depressed PTP. The defects in these longer-term forms of synaptic modulation also remain significant even if initial *lat* mutant synaptic transmission amplitude is reduced to the wild-type level by further reducing external Ca^{2+} . These results support the idea that LAT may have a specific role in the synaptic modulation mechanisms that support long-term augmentation and PTP at the NMJ. At the *Drosophila* NMJ, these more prolonged (minutes or longer) forms of plasticity have been shown to depend, at least in part, on the activation of cAMP and the cAMP-dependent signaling pathway (Zhong and Wu, 1991). In the presence of cAMP analogs, basal low-frequency stimulation reversibly induces prolonged (>30 min) potentiation. Tetanic stimulation accelerates PTP formation in the presence of cAMP, indicating the cAMP modulation process is also activity dependent (Zhong and Wu, 1991).

Learning and memory mutations known to alter cAMP synthesis and degradation also alter synaptic augmentation and potentiation properties (Zhong and Wu, 1991; Storm et al., 1998). In particular, the *Drosophila* mutants of *dunce*, which encodes a cAMP-specific phosphodiesterase (Byers et al., 1981), have increased cAMP levels and impaired olfactory learning and short-term memory (Tully and Gold, 1993; Davis et al., 1995; Dubnau and Tully, 1998). Both *dunce* and *lat* mutants display markedly similar functional phenotypes at the larval NMJ. In low external Ca^{2+} , *dunce* basal-evoked transmission is characterized by a strongly (4-fold over normal) elevated EJC amplitude, similar to the 3- to 4-fold increase observed for *lat*; and like *lat*, also has a reduced Ca^{2+} dependency of transmission (Zhong and Wu, 1991). Moreover, *dunce* mutant NMJs also show a nearly complete loss of STF, longer-term augmentation, and PTP (Zhong and Wu, 1991). The only striking difference between the *lat* and *dunce* mutant phenotypes is that *dunce* also significantly increases NMJ morphological growth, including bouton number and terminal branching, by 30%–50% (Zhong et al., 1992). The *lat* mutation is therefore of particular interest as a second example in which abnormally elevated synaptic transmission strength is correlated with a deleterious effect on learning or memory but that is unique among *Drosophila* learning/memory genes in that it appears to affect presynaptic function independently of morphology.

Parallel evidence that cAMP levels critically regulate long-term synaptic plasticity and memory formation comes from *Drosophila rutabaga* mutants, which have

reduced cAMP levels due to the loss of Ca^{2+} /CaM-dependent AC activity (Levin et al., 1992). Basal-evoked transmission amplitude at *rutabaga* mutant NMJs is normal, but STF and augmentation are weaker than normal, and mutants cannot sustain PTP (Zhong and Wu, 1991). Though the effect on cAMP level and synaptic phenotype are distinctly different, *rutabaga* and *dunce* mutants have similar defects in adult olfactory learning and memory ability (Davis et al., 1995; Dubnau and Tully, 1998). In mammals, the impaired cerebellar LTP observed for AC mutant mice (Storm et al., 1998) further demonstrates the importance of cAMP activation in learning and memory processes. These studies strongly suggest that cAMP elevation, activated at least in part by sustained presynaptic elevations of Ca^{2+} occurring during high-frequency activity, initiates the functional long-term synaptic potentiation necessary for normal learning and memory to occur. However, habitually elevated cAMP levels, as in *dunce* mutants, can result in permanently potentiated synapses without the ability to dynamically upregulate Ca^{2+} - and cAMP-dependent pathways, with equally negative behavioral consequences.

Evidence from *Drosophila*, *Aplysia*, and mice strongly indicate that the downstream effector of lasting cAMP-mediated functional and behavioral modifications is gene expression regulated by the CRE and CRE-binding protein, CREB (Bourtchuladze et al., 1994; Yin et al., 1994, 1995; Bailey et al., 1996; Impey et al., 1996; Goda, 1995a, 1995b; Yin and Tully, 1996). In *Drosophila*, the induced transgenic expression of activator or repressor isoforms of the *Drosophila* form of CREB (dCREB2) specifically enhances or blocks long-term memory formation, respectively (Yin et al., 1994, 1995). Expression of the dCREB2 repressor isoform during development in *dunce* mutant larvae also partially rescues the *dunce* mutant synaptic transmission and functional plasticity defects at the NMJ (Davis et al., 1996). These results suggest that the permanently altered plasticity at *dunce* mutant NMJs is indeed a consequence of the overexpression of genes under the transcriptional regulation of dCREB2, brought about by abnormally high levels of cAMP.

The *lat* mutant olfactory learning defect, combined with the striking functional similarities between the *lat* and *dunce* mutants, leads us to speculate that LAT may also be involved in cAMP-dependent forms of synaptic modulation. The behavioral defects of the viable *lat*^{P1} mutant appear to be specific to the initial acquisition or learning step rather than to subsequent forms of short- or long-term memory (Boynton and Tully, 1992). LAT may therefore function in one or more short-term, transcription-independent forms of modulation, including cAMP-dependent aspects of synaptic vesicle mobilization, docking, and release as well as downstream protein kinase A-dependent modulation of synaptic efficacy, or in another protein kinase or signal transduction pathway also involved in synaptic modulation.

Future work must focus on synaptic ultrastructural correlations to the *lat* mutant functional phenotype and the relationship of this pioneer synaptic protein to identified synaptic proteins and modulation pathways. Examination of mutant synaptic ultrastructure will be necessary to reveal alterations in the number or structure of presynaptic release sites and the availability of synaptic

vesicles at these sites. Ca^{2+} imaging at resting and stimulated synaptic terminals in *lat* mutants may provide insight into a possible function in presynaptic Ca^{2+} regulation. Involvement in cAMP-dependent synaptic modulation can be tested by examining functional synaptic transmission and plasticity in *lat* double mutant combinations with *dunce* and *rutabaga*. These studies, together with continued molecular analysis, promise to advance the understanding of LAT's molecular role.

Experimental Procedures

Drosophila Stocks

The recessive hypomorphic allele *lat*^{P1} was initially isolated in a P element mutagenesis screen for mutants showing 3 hr memory deficits in a Pavlovian olfactory learning assay (Boynton and Tully, 1992; Dura et al., 1993). A series of six lethal imprecise excision alleles (*lat*^{le34}, *lat*^{le49}, *lat*^{le107}, *lat*^{le344}, *lat*^{le352}, and *lat*^{le372}) was subsequently generated by mobilization of the *lat*^{P1} P element. Three additional lethal alleles (*lat*^{vr6.35}, *lat*^{vr6.6}, and *lat*^{vr6.r6}) were produced independently by EMS or γ ray mutagenesis (Lasko and Pardue, 1988). The lethal alleles fail to complement each other for adult viability, and all result in homozygous lethality in third instar or early pupal stages (Boynton and Tully, 1992; Boynton, 1993) except *lat*^{vr6.35}, which contains an embryonic lethal second site mutation (Boynton, 1993).

The viable learning mutant *lat*^{P1}, the excision alleles *lat*^{le49} and *lat*^{le344}, and the EMS-induced lethal allele *lat*^{vr6.6} were selected for this study. Western blots of *lat*^{le344}/*lat*^{le344} larval extracts with an anti-LAT antibody reveal no LAT protein expression. Furthermore, we detect little or no LAT protein expression in situ in homozygous *lat*^{le49}, *lat*^{le344}, or *lat*^{vr6.6} larvae, and all three alleles show nearly identical mutant synaptic transmission phenotypes. We therefore consider these three alleles to be very strong hypomorphs or null mutants and refer to them here collectively as *lat*⁻.

Fly stocks were reared on standard cornmeal food at 25°C. Balanced stocks carrying the lethal *lat* alleles (*w;lat*⁻ *CyO*) were crossed either to *yw;sco/CyO y*⁺ or *leo¹¹⁸⁸/SM5-TM6B Tb* flies to generate new balanced stocks *yw;lat*⁻/*CyO y*⁺ and *lat*⁻/*SM5-TM6B Tb*. For immunohistological staining and electrophysiological experiments, adult flies were transferred to a fresh tube and allowed to mate for 8–24 hr. Homozygous *lat*⁻/*lat*⁻ larvae were identified by the markers *y*⁻ (for *yw;lat*⁻/*CyO y*⁺-balanced stocks) or *Tb*⁺ (for *lat*⁻/*SM5-TM6B Tb*-balanced stocks). By late third instar (5–6 days AEL), *lat*⁻ larvae were found at about half the expected 1:3 ratio, indicating this age overlaps the lethal phase. Mutant larvae selected for experiments were size matched with control wild-type larvae (Oregon R). Well-developed larvae (~6 days AEL) were selected that had either left the food ("wandering" stage) or remained in the food but had reached the prominent size characteristic of wild-type wandering third instar larvae.

Generation of *lat*^{le344}/*lat*^{le344};*glat*⁺ 3-1/+ Transgenic Flies

Transgenic flies were generated as described by Pinto et al. (1999). Briefly, a 17.1 kb NotI restriction fragment containing the entire *lat* transcription unit was cloned into the NotI site of a CaSper-2 vector (Thummel and Pirrotta, 1991). This *glat*⁺ genomic construct was injected into *w¹¹¹⁹* (isoCJ1) embryos. Independent *glat*⁺ insertions were mapped to separate chromosomes using *w;CyO/Sp;TM3,Ser/Sb* flies. The *glat*⁺ line, containing a *glat*⁺ insertion on the third chromosome, was crossed into a *lat* null mutant (*lat*^{le344}/*lat*^{le344}) background. Female *lat*^{le344}/*CyO* flies were crossed to *CyO/Sp;glat*⁺/*TM3,Ser* males. The *lat*^{le344}/*CyO;glat*⁺ 3-1/+ progeny were then crossed to each other to yield *lat*^{le344}/*lat*^{le344} (*CyO*⁺, *Ser*⁺) offspring carrying either one or two copies of *glat*⁺ 3-1. Flies with a single copy (*lat*^{le344}/*lat*^{le344};*glat*⁺ /+) were produced from this cross at a ratio close to that expected for complete rescue of the lethality-associated null *lat* genotype. Few flies with two copies (*lat*^{le344}/*lat*^{le344};*glat*⁺ /*glat*⁺ 3-1) were produced, suggesting a deleterious effect resulting either from two copies of *glat*⁺ 3-1 or from homozygosity of the insertion site (Pinto et al., 1999). Third instar larval progeny (5–6 days AEL) from *lat*^{le344}/*lat*^{le344};*glat*⁺ /+ flies were used for electrophysiological recordings in rescue experiments.

Antibody Purification and Immunohistology

A rabbit polyclonal antibody was raised against the LAT protein. The protein was expressed bacterially from a pET vector containing nucleotide sequence corresponding to the first 658 amino acids of the complete 671 amino acid LAT sequence (Pinto et al., 1999). The antiserum was affinity purified with nitrocellulose-bound LAT antigen. The affinity-purified antiserum (1:10 dilution) recognizes a single 79 kDa band on Western blots of wild-type larval CNS protein extracts. No corresponding band is detected in CNS protein extracts from null mutant (*lat*^{vr6.6}/*lat*^{le344} or *lat*³⁴⁴/*lat*^{le344}) larvae.

Larval preparations were fixed and immunohistologically stained as reported previously (Broadie and Bate, 1993; Broadie et al., 1995). Briefly, third instar larvae were dissected along the dorsal midline in Ca^{2+} -free saline, pinned flat in sylgard-coated petri dishes, and fixed for 45–75 min with 4% paraformaldehyde in phosphate-buffered saline (PBS). Following fixation, preparations were washed three times (10 min/wash) in PBS-TX (0.1% Triton X-100 in PBS) containing 5 mg/ml bovine serum albumin. All antibody incubations and subsequent washes were carried out in PBS-TX. Primary antibody incubations were carried out overnight at 4°C followed by incubation with an appropriate biotinylated or fluorescent secondary antibody (1:300 to 1:500 dilutions) for 2 hr at room temperature.

A mouse monoclonal anti-CSP antibody (1:10 dilution) was used to examine wild-type and mutant NMJ morphology. Staining was carried out using a Vectastain ABC Elite kit (Vector Laboratories, Burlingame, CA) with diaminobenzidine (DAB) reaction and $NiCl_2$ or $NiCl_2/CoCl_2$ enhancement, as reported previously (Broadie and Bate, 1993; Broadie et al., 1995, 1997). Preparations were then dehydrated by an ethanol series, cleared in HistoClear, and mounted in araldite. NMJs were visualized with Nomarski optics at 1000 \times on a Zeiss Axioskop microscope. Images of representative terminals were collected with a digital camera and Spot image acquisition software (Ziess). To examine LAT localization, wild-type and *lat*⁻ mutant larvae were incubated with anti-LAT antiserum (1:10), stained by the DAB technique, and mounted and visualized as above. Single and double fluorescent antibody-labeling experiments were also used to examine LAT localization alone or in combination with other known pre- and postsynaptic proteins. For these experiments, wild-type preparations were incubated with anti-LAT alone or with anti-LAT followed by either anti-CSP, rat monoclonal anti-Dlg (1:500), or mouse monoclonal anti- β PS integrin (1:100) except for glutamate receptor double-staining experiments, in which a monoclonal mouse anti-*myc* (1:500) was used to stain larvae expressing *myc*-tagged DGLuR2a protein (Petersen et al., 1997). Preparations were stained with secondary antibodies (1:300 to 1:500) with avidin-conjugated fluorochrome and mounted in 70% glycerol or Vectashield (Vector Laboratories) mounting medium. Optical sections of the neuromusculature were collected for analysis with a BioRad MRC 600 confocal microscope. Color images and microscopy figures were constructed with Adobe Photoshop software.

To analyze synaptic terminal branching and bouton number, anti-CSP-stained NMJs in wild-type and *lat*⁻ mutant larvae were visualized at 1000 \times . Terminal branch segments for muscles 12 and 4 in segment A2 on both sides of the animal were schematically sketched by hand. Branch segments were classified and counted by methods similar to those described by Wang et al. (1994) and Zhong et al. (1992). Muscle 12 is innervated by several motor axons, each of which forms synaptic boutons of a different morphological class (type Ib, Is, II, or III) (Johansen et al., 1989; Gorczyca et al., 1993; Jia et al., 1993). Although we did not count each bouton type individually, at most terminals, it was possible to distinguish one or two primary branches, usually one anterior and one posterior, for each class of bouton. Branches originating directly from the nerve entry point onto the muscle were classified as primary branches. Each subsequent branch fork defined progressively higher-order segments (secondary, tertiary, etc.). A branch was defined as a length of terminal with two or more boutons. At muscle 4, several distinct inputs or insertions were usually observed, including one or more terminals of smaller boutons formed by more dorsal nerve projections. Only the prominent principal NMJ, usually formed near the center of the fiber and containing type Ib boutons, was analyzed. The total number of synaptic boutons at muscles 12, 4, and 6/7 was counted on both sides of the preparation in segment A2.

Electrophysiology

Electrophysiological recordings were made at 18°C from muscle 12 or muscle 6 in the anterior ventral abdomen (A2–A5; primarily A3)

of wild-type and mutant wandering third instar larvae (~6 days AEL), using standard TEVC techniques (Zhong and Wu, 1991). Dissections and recordings were made in a modified version of standard *Drosophila* saline (Jan and Jan, 1976a; Zhong and Wu, 1991) containing additional sucrose (34 mM) as well as 5 mM trehalose. The final saline composition was (in mM): NaCl, 128; KCl, 2; MgCl₂, 4; trehalose, 5; sucrose, 70; and HEPES, 5 (pH adjusted to 7.1 with NaOH). The addition of sucrose approximated the osmotic strength reported in natural haemolymph (Stewart et al., 1994) and seemed to alleviate muscle vacuolation. Larvae were secured at the head and tail to sylgard- (Dow Corning) coated glass coverslips with histoacryl tissue adhesive glue (Braun, Germany) in low-Ca²⁺ (0.1–0.2 mM) containing saline and dissected along the dorsal midline with fine dissection scissors. The cuticle was glued flat to the coverslip, and the internal organs and fat bodies were removed to expose the CNS and ventral muscles. The segmental nerves of all preparations were severed near the CNS to eliminate junctional responses originating from CNS activity. The dissection saline was replaced with fresh recording saline containing CaCl₂ at final concentrations of 0.1–1.0 mM. Preparations were visualized with a 40× water immersion objective on a Zeiss Axioskop microscope equipped with Nomarski optics.

Evoked EJC were recorded in the voltage-clamped muscle (V_{hold} , –60 mV) by stimulating (0.25–1 ms) the segmental nerve with a fire-polished suction electrode filled with extracellular saline. Intracellular microelectrodes were pulled (Sutter P-97, Sutter Instruments) from 1 mm outer diameter glass capillaries (World Precision Instruments) containing an internal filament. Voltage recording electrodes were filled with 3 M KCl and had resistances of 15–40 MΩ. Current-passing electrodes were filled with a 3:1 mixture of 3 M K⁺ acetate to KCl (Stewart et al., 1994) and had resistances of 12–25 MΩ. EJCs were recorded with an Axoclamp 2B amplifier (Axon Instruments, Burlingame, CA) in TEVC mode. After establishing TEVC, a 10 mV hyperpolarizing command pulse was applied. The clamp feedback gain, capacitance neutralization, and speed controls were advanced so that the peak amplitude and kinetics of the current transient were maximal without introducing oscillations or excess noise. The intracellularly recorded voltage during the EJC was also examined on an oscilloscope, and the gain was further adjusted to minimize the deviation from the command voltage (–60 mV) at the peak current. For lower Ca²⁺ concentrations, at which most of the recordings were done, EJCs were smaller (2–40 nA), and maximum voltage deviations were a few mV or less. At higher external Ca²⁺ (0.4–1.0 mM), maximum voltage deviations of 5–6 mV occurred only for EJCs of 100 nA or larger; the clamp quality and voltage control were judged by these criteria to be adequate. Spontaneous mEJCs were recorded continuously (gap-free recording mode) in muscle 12 at –80 mV in 0.1 mM Ca²⁺.

Current signals were filtered at 500–1000 Hz and digitized directly to disk with PClamp6 acquisition hardware and software (Axon Instruments). For continuous recordings of EJCs in PTP experiments and mEJCs, synaptic currents were captured with event detection and analysis software (ACSPLOUF) written and kindly provided by Dr. P. Vincent and described elsewhere (Vincent and Marty, 1993). Exemplar EJC traces were averaged from 5–20 consecutive individual responses except for the individual events shown in Figures 6A, 7E, and 8E. EJC and mEJC amplitude analysis, event averaging, and statistical analysis were carried out using PClamp6 analysis and commercial spreadsheet software. Individual and averaged traces were exported to standard graphics programs for figure presentation. All data are presented as mean ± SEM unless otherwise indicated.

Acknowledgments

We are grateful to K. Zinsmaier, N. Brown, and V. Budnik for providing antibodies to CSP, βPS integrin, and Dlg, respectively; to C. Goodman for providing fly stocks expressing myc-tagged glutamate receptors; to E. Jorgensen and T. Fergestad for critical comments on the manuscript; to D. Yoshikami and J. Renger for helpful experimental suggestions; to E. King for assistance with confocal microscopy and image processing; and to E. Rushton for invaluable and expert technical assistance. This work was supported by National

Institutes of Health grant NS32480 and a grant from the John A. Hartford Foundation (T. T.) and by National Institutes of Health grant GM54544, a Sloan Fellowship, a Searle Scholar Award, and a Young Investigator Award from the Office of Naval Research (K. B.).

Received February 23, 1998; revised March 9, 1999.

References

- Abel, T., Nguyen, P.V., Barad, M., Deuel, T.A., Kandel, E.R., and Bourchuladze, R. (1997). Genetic demonstration of a role for PKA in the late phase of LTP and in hippocampal-based long-term memory. *Cell* 88, 615–626.
- Aitken, A. (1995). 14–3–3 proteins on the MAP. *Trends Biochem. Sci.* 20, 95–97.
- Alnaes, E., and Rahamimoff, R. (1975). On the role of mitochondria in transmitter release from motor nerve terminals. *J. Physiol. (Lond)* 248, 285–306.
- Anderson, M.S., Halpern, M.E., and Keshishian, H. (1988). Identification of the neuropeptide transmitter proctolin in *Drosophila* larvae: characterization of muscle fiber-specific neuromuscular endings. *J. Neurosci.* 8, 242–255.
- Atwood, H.L., Govind, C.K., and Wu, C.-F. (1993). Differential ultrastructure of synaptic terminals on ventral longitudinal abdominal muscles in *Drosophila* larvae. *J. Neurobiol.* 24, 1008–1024.
- Bailey, C.H., Bartsch, D., and Kandel, E.R. (1996). Toward a molecular definition of long-term memory storage. *Proc. Natl. Acad. Sci. USA* 93, 13445–13452.
- Bernabeu, R., Bevilacqua, L., Ardenghi, P., Bomberg, E., Schmitz, P., Bianchin, M., Izquierdo, I., and Medina, J.H. (1997). Involvement of hippocampal cAMP/cAMP-dependent protein kinase signaling pathway in a late memory consolidation phase of aversively motivated learning in rats. *Proc. Natl. Acad. Sci. USA* 94, 7041–7046.
- Bolwig, G.M., Del Vecchio, M., Hannon, G., and Tully, T. (1995). Molecular cloning of *linotte* in *Drosophila*: a novel gene that functions during associative learning. *Neuron* 15, 829–842.
- Bourchuladze, R., Freguelli, B., Blendy, J., Cioffi, D., Schultz, G., and Silva, A.J. (1994). Deficient long-term memory in mice with a targeted mutation of the cAMP-responsive element-binding protein. *Cell* 79, 59–68.
- Boynton, S., and Tully, T. (1992). *latheo*, a new gene involved in associative learning and memory in *Drosophila melanogaster*, identified from P element mutagenesis. *Genetics* 132, 655–672.
- Boynton, S.C. (1993). Behavioral genetic studies on learning and memory in *Drosophila melanogaster*. PhD thesis, Brandeis University, Waltham, Massachusetts.
- Broadie, K., and Bate, M. (1993). Development of the embryonic neuromuscular synapse of *Drosophila melanogaster*. *J. Neurosci.* 13, 144–166.
- Broadie, K., Prokop, A., Bellen, H.J., O’Kane, C.J., Schulze, K.L., and Sweeney, S.T. (1995). Syntaxin and synaptobrevin function downstream of vesicle docking in *Drosophila*. *Neuron* 15, 663–673.
- Broadie, K., Rushton, E., Skoulakis, E.M.C., and Davis, R.L. (1997). Leonardo, a *Drosophila* 14–3–3 protein involved in learning, regulates presynaptic function. *Neuron* 19, 391–402.
- Byers, D., Davis, R.L., and Kiger, J.A. (1981). Defect in cyclic AMP phosphodiesterase due to the dunce mutation of learning in *Drosophila melanogaster*. *Nature* 289, 79–81.
- David, G., Barrett, J.N., and Barrett, E.F. (1998). Evidence that mitochondria buffer physiological Ca²⁺ loads in lizard motor nerve terminals. *J. Physiol. (Lond)* 509, 59–65.
- Davis, G.W., Schuster, C.M., and Goodman, C.S. (1996). Genetic dissection of structural and functional components of synaptic plasticity. III. CREB is necessary for presynaptic functional plasticity. *Neuron* 17, 669–679.
- Davis, R.L. (1996). Physiology and biochemistry of *Drosophila* learning. *Physiol. Rev.* 76, 299–317.
- Davis, R.L., Cherry, J., Dauwalder, B., Han, P.L., and Skoulakis,

- E.M.C. (1995). The cyclic AMP system and *Drosophila* learning. *Mol. Cell. Biochem.* 149–150, 271–278.
- Delgado, R., Latorre, R., and Labarca, P. (1992). K(+) -channel blockers restore synaptic plasticity in the neuromuscular junction of *dunce*, a *Drosophila* learning and memory mutant. *Proc. R. Soc. Lond. B Biol. Sci.* 250, 181–185.
- DeZazzo, J., and Tully, T. (1995). Dissection of memory formation: from behavioral pharmacology to molecular genetics. *Trends Neurosci.* 18, 212–218.
- Dubnau, J., and Tully, T. (1998). Gene discovery in *Drosophila*: new insights for learning and memory. *Annu. Rev. Neurosci.*, in press.
- Dura, J.M., Preat, T., and Tully, T. (1993). Identification of *linotte*, a new gene affecting learning and memory in *Drosophila melanogaster*. *J. Neurogenet.* 9, 1–14.
- Fischer, S.A., Fischer, T.M., and Carew, T.J. (1997). Multiple overlapping processes underlying short-term synaptic enhancement. *Trends Neurosci.* 20, 170–177.
- Fossier, P., Baux, G., and Tauc, L. (1993). Role of different types of Ca²⁺ channels and a reticulum-like Ca²⁺ pump in neurotransmitter release. *J. Physiol. (Paris)* 87, 3–14.
- Fossier, P., Deibler, M.F., Mothet, J.P., Israel, M., Tauc, L., and Baux, G. (1998). Control of the calcium concentration involved in acetylcholine release and its facilitation: an additional role for synaptic vesicles? *Neuroscience* 85, 85–91.
- Frey, U., Huang, Y.Y., and Kandel, E.R. (1993). Effects of cAMP simulate a late stage of LTP in hippocampal CA1 neurons. *Science* 260, 1661–1664.
- Goda, Y. (1995a). Memory mechanisms. A common cascade for long-term memory. *Curr. Biol.* 5, 136–138.
- Goda, Y. (1995b). Memory mechanisms. Photographic memory in flies. *Curr. Biol.* 5, 852–853.
- Goodwin, S.F., Del Vecchio, M., Velinzon, K., Hogell, C., Russel, S.R., Tully, T., and Kaiser, K. (1997). Defective learning in mutants of the *Drosophila* gene for a regulatory subunit of cAMP-dependent protein kinase. *J. Neurosci.* 17, 8817–8827.
- Gorczyca, M., Augart, C., and Budnik, V. (1993). Insulin-like receptor and insulin-like peptide are localized at neuromuscular junctions in *Drosophila*. *J. Neurosci.* 13, 3692–3704.
- Grotewiel, M.S., Beck, C.D.O., Wu, K.H., Zhu, X.-R., and Davis, R.L. (1998). Integrin-mediated short-term memory in *Drosophila*. *Nature* 391, 455–460.
- Hawkins, R.D., Kandel, E.R., and Siegelbaum, S.A. (1993). Learning to modulate transmitter release: themes and variations in synaptic plasticity. *Annu. Rev. Neurosci.* 16, 625–665.
- Impey, S., Mark, M., Villacres, E.C., Poser, S., Chavkin, C., and Storm, D.R. (1996). Induction of CRE-mediated gene expression by stimuli that generate long-lasting LTP in area CA1 of the hippocampus. *Neuron* 16, 973–982.
- Jan, L.Y., and Jan, Y.N. (1976a). Properties of the larval neuromuscular junction in *Drosophila melanogaster*. *J. Physiol. (Lond)* 262, 189–214.
- Jan, L.Y., and Jan, Y.N. (1976b). L-glutamate as an excitatory transmitter at the *Drosophila* larval neuromuscular junction. *J. Physiol. (Lond)* 262, 215–236.
- Jia, X., Gorczyca, M., and Budnik, V. (1993). Ultrastructure of neuromuscular junctions in *Drosophila*: comparison of wild-type and mutants with increased excitability. *J. Neurobiol.* 24, 1025–1044.
- Johansen, J., Halpern, M.E., Johansen, K.M., and Keshishian, H. (1989). Stereotypic morphology of glutamatergic synapses on identified muscle cells of *Drosophila* larvae. *J. Neurosci.* 9, 710–725.
- Kamiya, H., and Zucker, R.S. (1994). Residual Ca²⁺ and short-term plasticity. *Nature* 371, 603–606.
- Kandel, E.R., and Schwartz, J.H. (1982). Molecular biology of learning: modulation of transmitter release. *Science* 218, 433–443.
- Keshishian, H., Chiba, A., Chang, T.N., Halfon, M.S., Harkins, E.W., Jarecki, J., Wang, L., Anderson, M.S., Cash, S., Halpern, M.E., and Johansen, J. (1993). Cellular mechanisms governing synaptic development in *Drosophila melanogaster*. *J. Neurobiol.* 24, 757–787.
- Lasko, P.F., and Pardue, M.L. (1988). Studies of the genetic organization of the vestigial microregion of *Drosophila melanogaster*. *Genetics* 120, 495–502.
- Levin, I.R., Han, P.-L., Hwang, P.M., Feinstein, P.G., Davis, R.L., and Redd, R.R. (1992). The *Drosophila* learning and memory gene *rutabaga* encodes a Ca²⁺/calmodulin-responsive adenylyl cyclase. *Cell* 68, 479–489.
- Monastirioti, M., Gorczyca, M., Rapus, J., Eckart, M., White, K., and Budnick, V. (1995). Octopamine immunoreactivity in the fruit fly *Drosophila melanogaster*. *J. Comp. Neurol.* 356, 275–287.
- Nguyen, P.V., Abel, T., and Kandel, E.R. (1994). Requirement of a critical period of transcription for induction of a late phase of LTP. *Science* 265, 1104–1107.
- Petersen, S.A., Fetter, R.D., Noordermeer, J.N., Goodman, C.S., and DiAntonio, A. (1997). Genetic analysis of glutamate receptors in *Drosophila* reveals a retrograde signal regulating presynaptic transmitter release. *Neuron* 19, 1237–1248.
- Pinto, S., Quintana, D.G., Smith, P., Mihalek, R.M., Hou, Z.-H., Boynton, S., Jones, C.J., Hendricks, M., Velinzon, K., Wohlschlegel, J.A., et al. (1999). *latheo* encodes a subunit of the origin recognition complex and disrupts neuronal proliferation and adult olfactory memory when mutant. *Neuron* 23, this issue, 45–54.
- Skoulakis, E.M.C., and Davis, R.L. (1996). Olfactory learning deficits in mutants for *leonardo*, a *Drosophila* gene encoding a 14–3–3 protein. *Neuron* 17, 931–944.
- Stewart, B.A., Atwood, H.L., Renger, J.J., Wang, J., and Wu, C.-F. (1994). Improved stability of *Drosophila* larval neuromuscular preparations in haemolymph-like physiological solutions. *J. Comp. Physiol.* 175, 179–181.
- Storm, D.R., Hansel, C., Hackler, B., Parent, A., and Linden, D.J. (1998). Impaired cerebellar long-term potentiation in type I adenylyl cyclase mutant mice. *Neuron* 20, 1199–1210.
- Tang, Y., and Zucker, R.S. (1997). Mitochondrial involvement in post-tetanic potentiation of synaptic transmission. *Neuron* 18, 483–491.
- Thummel, C.S., and Pirrotta, V. (1991). Technical notes: new pCaSpeR P-element vectors. *Drosophila Inform. Newslett.* 2 (gopher://flybase.bio.indiana.edu:70/11/docs/news/DIN).
- Tully, T. (1997). Regulation of gene expression and its role in long-term memory and plasticity. *Proc. Natl. Acad. Sci. USA* 94, 4239–4241.
- Tully, T., and Gold, D. (1993). Differential effects of *dunce* mutations on associative learning and memory in *Drosophila*. *J. Neurogenet.* 9, 55–71.
- Tully, T., and Quinn, W.G. (1985). Classical conditioning and retention in normal and mutant *Drosophila melanogaster*. *J. Comp. Physiol. (A)* 157, 263–277.
- Tully, T., Preat, T., Boynton, S.C., and Del Vecchio, M. (1994). Genetic dissection of consolidated memory in *Drosophila*. *Cell* 79, 35–47.
- Vincent, P., and Marty, A. (1993). Neighboring cerebellar Purkinje cells communicate via retrograde inhibition of common presynaptic interneurons. *Neuron* 11, 885–893.
- Wang, J., Renger, J.J., Griffith, L.C., Greenspan, R.J., and Wu, C.-F. (1994). Comcomitant alterations of physiological and developmental plasticity in *Drosophila* CaM Kinase II-inhibited synapses. *Neuron* 13, 1373–1384.
- Yin, J.C., and Tully, T. (1996). CREB and the formation of long-term memory. *Curr. Opin. Neurobiol.* 6, 264–268.
- Yin, J.C., Wallach, J.S., Del Vecchio, M., Wilder, E.L., Zhou, H., Quinn, W.G., and Tully, T. (1994). Induction of a dominant negative CREB transgene specifically blocks long-term memory in *Drosophila*. *Cell* 79, 49–58.
- Yin, J.C., Del Vecchio, M., Zhou, H., and Tully, T. (1995). CREB as a memory modulator: induced expression of a dCREB activator isoform enhances long-term memory in *Drosophila*. *Cell* 81, 107–115.
- Zhao, M.L., and Wu, C.-F. (1997). Alterations in frequency coding and activity dependence of excitability in cultured neurons of *Drosophila* memory mutants. *J. Neurosci.* 17, 2187–2199.
- Zhong, Y., and Wu, C.-F. (1991). Altered synaptic plasticity in *Drosophila* memory mutants with a defective cyclic AMP cascade. *Science* 251, 198–201.

Zhong, Y., and Wu, C.-F. (1993). Differential modulation of potassium currents by cAMP and its long-term and short-term effects: *dunce* and *rutabaga* mutants of *Drosophila*. *J. Neurogenet.* *9*, 15–27.

Zhong, Y., Budnik, V., and Wu, C.-F. (1992). Synaptic plasticity in *Drosophila* memory and hyperexcitable mutants: role of cAMP cascade. *J. Neurosci.* *12*, 644–651.

Zinsmaier, K.E., Eberle, K.K., Buchner, E., Walter, N., and Benzer, S. (1994). Paralysis and early death in cysteine string protein mutants of *Drosophila*. *Science* *263*, 977–980.

Zucker, R.S. (1993). Calcium and transmitter release. *J. Physiol. (Paris)* *87*, 25–36.

Zucker, R.S. (1996). Exocytosis: a molecular and physiological perspective. *Neuron* *17*, 1049–1055.